Quaternary Science Reviews 98 (2014) 110–125

Contents lists available at ScienceDirect

Quaternary Science Reviews

journal homepage: www.elsevier.com/locate/quascirev

Rock-magnetic signature of precipitation and extreme runoff events in south-eastern Patagonia since 51,200 cal BP from the sediments of Laguna Potrok Aike

A. Lisé-Pronovost [a, b, *], G. St-Onge [a, b], C. Gogorza [c], G. Jouve [b, d], P. Francus [b, d], B. Zolitschka [e], the PASADO Science Team

[a] Canada Research Chair in Marine Geology, Institut des sciences de la mer de Rimouski, Université du Québec à Rimouski, Rimouski, Canada
[b] GEOTOP Research Center, Montréal, Canada
[c] Centro de Investigaciones en Física e Ingeniería del Centro de la Provincia de Buenos Aires (CIFICEN-CONICET), Tandil, Argentina
[d] Centre Eau, Terre et Environnement, Institut National de la Recherche Scientifique, Québec, Québec, Canada
[e] GEOPOLAR, Institute of Geography, University of Bremen, Bremen, Germany

ARTICLE INFO

Article history:
Received 7 February 2014
Received in revised form
29 May 2014
Accepted 30 May 2014
Available online 23 June 2014

Keywords:
Rock magnetism
Laguna Potrok Aike
Lacustrine sediment
Paleoenvironment
Mass movement deposit
Gyroremanent magnetization

ABSTRACT

A 106-m long sediment sequence from the maar lake Laguna Potrok Aike in southern Patagonia was recovered in the framework of the International Continental Scientific Drilling Program (ICDP) Potrok Aike maar lake Sediment Archive Drilling prOject (PASADO). About half of the sedimentary sequence is composed of mass movement deposits (MMDs) and the event-corrected record reaches back to 51,200 cal BP. Here we present a high-resolution rock-magnetic study revealing two sedimentary facies associated with MMDs and characterized by two different types of spurious gyroremanent magnetization (GRM) acquired during static alternating field demagnetization. The first rock-magnetic signature is detected in MMDs composed of reworked sand and tephra material. The signature consists of GRM acquired during demagnetization of the natural remanent magnetization (NRM) and other rock-magnetic properties typical of iron sulfides such as greigite. We interpret these intervals as authigenic formation of iron sulfides in suboxic conditions within the MMD. The second rock-magnetic signature consists of a series of 10 short intervals located on the top of MMDs characterized by GRM acquisition during demagnetization of the isothermal remanent magnetization (IRM). Based on geological, limnological, stratigraphic and climatic evidence these layers are interpreted as reflecting pedogenic hematite and/or goethite brought to the lake by runoff events related to precipitation and permafrost melt. The pedogenic iron minerals mobilized from the catchment most likely settled out of suspension on top of MMDs after a rapid remobilization event. The series of runoff events corresponds to periods of increased lacustrine productivity in Laguna Potrok Aike and are coeval within the limit of the chronology to warm periods of the Last Glacial as recorded in Antarctica, the deglaciation in the mid-latitudes of the Southern Hemisphere and enhanced precipitation during the Early Holocene in southeastern Patagonia.

1. Introduction

Millennial-scale climate change recorded in Antarctica ice cores during the Last Glacial period led changes in Greenland (e.g., EPICA community members, 2006) and the last climatic transition was probably triggered in the Southern Hemisphere by the action of changing westerly winds (Anderson et al., 2009) or sea-ice cover (Knorr and Lohmann, 2003) on ocean circulation. Despite its importance in the global climate system, the pre-Holocene Antarctic millennial-scale climate variability remains less documented than its Greenland counterpart (e.g., Dansgaard/Oeschger events). This limitation is partly due to the scarcity of pre-Holocene high-resolution records in the Southern Hemisphere largely dominated by the open ocean. Nevertheless, in recent years a growing number of high-resolution paleoclimate records from the Southern Hemisphere emerged and revealed in-phase climate patterns with Antarctica, including marine sediment cores from offshore Australia and New Zealand (e.g., Pahnke, 2003; Barrows et al.,

* Corresponding author. Present address: The Australian Archeomagnetism Laboratory (TAAL), La Trobe University, Melbourne, Australia. Tel.: +61 03 9479 1392; fax: +61 3 9479 1881.
E-mail addresses: A.Lise-Pronovost@latrobe.edu.au, agathe_lp@hotmail.com (A. Lisé-Pronovost).

http://dx.doi.org/10.1016/j.quascirev.2014.05.029
0277-3791/

2007), southern South America (e.g. Kaiser et al., 2007; Caniupán et al., 2011; Weber et al., 2012) and in the path of the Antarctic circum-polar current (Mazaud et al., 2007; Pugh et al., 2009). Continental records from Australia (Williams et al., 2009), southern Africa (Gasse et al., 2008) and southern South America (Kilian and Lamy, 2012) also document Antarctic-like climate changes during the Last Glacial, however generally at low temporal resolution and often discontinuously.

The Potrok Aike maar lake Sediment Archive Drilling prOject (PASADO) in the framework of the International Continental Scientific Drilling Program (ICDP) recovered a high-resolution sedimentary archive reaching back to the Last Glacial in southern South America (Zolitschka et al., 2009, 2013 and papers therein). Previous records from this region are mostly limited to the Holocene and the Lateglacial (cf. Kilian and Lamy, 2012). Located in a region identified as the source area for Glacial dust deposited in Antarctica during the Last Glacial periods (Basile et al., 1997), the new continental record from Laguna Potrok Aike provides a unique opportunity to document past climate changes in south-eastern Patagonia since the Last Glacial period for comparison with the Antarctic climate record.

Careful macroscopic sedimentological study of the long PASADO sedimentary sequence revealed that mass movement deposits (MMD) including ball and pillow structures, normally graded beds, structureless sands and fine gravel layers constitute about half of the record (Kliem et al., 2013a,b). Recent geochemical, mineralogical and elemental studies indicate rare diagenetic remobilization linked to oxic conditions and only sparse organic and carbonate inputs (Hahn et al., submitted for publication; Nuttin et al., 2013). Despite a relatively homogeneous clastic composition throughout the sedimentary sequence, Jouve et al. (submitted for publication) documented identical geochemical signatures for different types of microfacies and as a result, Jouve et al. (2013; submitted for publication) and Hahn et al. (submitted for publication) raised caution against the use of some elemental ratios (e.g., Fe/Mn, Fe/Ti, Mn/Ti) to infer paleoclimatic changes on the complete sequence. In addition, the presence of micropumice (Jouve et al., 2013) and fine sands to coarse silt layers disseminated throughout the record (Kliem et al., 2013a,b) highlight the difficulty for readily identifying some MMD and for interpreting paleoclimatic signals.

Magnetic properties of the sediment appear especially suited to overcome these difficulties and build continuous paleoclimate proxies from the sediments of Laguna Potrok Aike. Magnetic properties have the advantage of targeting only magnetic mineral (primarily iron oxides, oxyhydroxides and sulfides) and they are not necessarily biased by dilution effects such as the presence of rhyolitic micropumice in Laguna Potrok Aike (Jouve et al., 2013; Wastegård et al., 2013). Mineralogy and grain size-dependent magnetic properties are not influenced by concentration changes, and concentration-dependent parameters can be normalized to avoid such influences (Verosub and Roberts, 1995; Dekkers, 1997; Maher and Thompson, 1999; Evans and Heller, 2003). Previous rock-magnetic measurements from the sediments of Laguna Potrok Aike indicate a magnetic assemblage dominated by magnetite (Gogorza et al., 2011, 2012; Recasens et al., 2012; Lisé-Pronovost et al., 2013; submitted for publication). But evidence for other iron oxides such as maghemite and/or hematite (Gogorza et al., 2012), as well as iron sulfides (Jouve et al., 2013; Vuillemin et al., 2013) were reported. The low-resolution analyses of the PASADO core-catcher samples recently uncovered the potential to use rock-magnetism to identify MMD (Recasens et al., 2012). Here we present a high-resolution rock-magnetic study of the complete sedimentary sequence from Laguna Potrok Aike in order to investigate changes in the magnetic assemblage associated with MMDs and discuss their paleoclimatic implications.

2. Geological setting

Laguna Potrok Aike (51°58′S, 70°23′W; 113 m a.s.l.) is the only maar lake in the Pali Aike volcanic field in southern Argentina (Fig. 1A), with a maximum diameter of 3.5 km and water depth of 100 m. Located on the lee-side of the Andean cordillera in south-eastern Patagonia, the region is today influenced by the strong, dry and persistent Southern Hemisphere Westerly Winds (SWW) (e.g., Garreaud et al., 2013). As a result, the annual precipitation is low (ca 200 mm/yr; Mayr et al., 2007; Ohlendorf et al., 2013), the climate is semi-arid and aridisols are capable of holding only sparse Patagonian steppe vegetation (Wille et al., 2007; Schäbitz et al., 2013). Winds rarely originate from other directions but easterly winds from the humid Atlantic air masses can be accompanied by

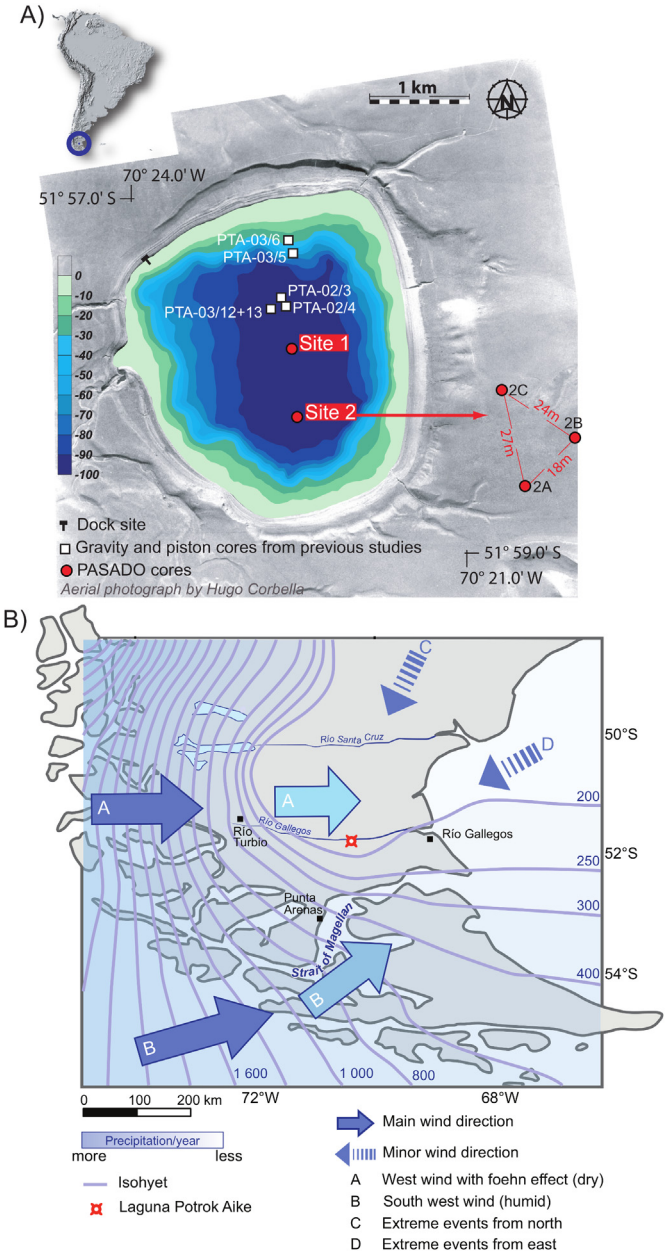

Fig. 1. A) Aerial photograph and bathymetry of Laguna Potrok Aike in southern South America. The PASADO coring sites 1 and 2 as well as other coring sites discussed in the text are indicated. B) Main and minor wind directions as well as annual precipitation in southern South America (modified from Schäbitz et al., 2013).

extreme precipitation events (Ohlendorf et al., 2013; Schäbitz et al., 2013) (Fig. 1B). The lake is polymictic; there is currently no stratification of the water column (Zolitschka et al., 2006) and recent high-resolution geochemical study revealed that such oxic conditions have predominated since 51,200 cal yr BP (Hahn et al., submitted for publication). Both aerial and submerged lake level terraces indicate significant lake level changes have occurred since the Last Glacial period (Haberzettl et al., 2005, 2008; Kliem et al., 2013a,b; Zolitschka et al., 2013). At present there is no inflow or outflow and the clastic lacustrine sediment is primarily deposited after eolian transport, and subordinated by remobilization of sediments during lake level changes and episodic runoff event.

The regional surface geology consists of semi-consolidated sedimentary rocks of the Miocene Santa Cruz Formation, Mio-Pliocene basalts, pyroclastic and phreatomagmatic sediments, and unconsolidated Quaternary deposits including tills, glaciofluvial, fluvial, lacustrine and aeolian sediments (D'Orazio et al., 2000; Zolitschka et al., 2006; Ross et al., 2011; Coronato et al., 2013). The unconsolidated deposits provide abundant silt to sand size detrital magnetite (Coronato et al., 2013; Lisé-Pronovost et al., 2013; submitted for publication).

3. Methods

3.1. Field work

A total of 533 m of sediment were retrieved in 2008 at two sites in the deep basin of Lake Laguna Potrok Aike (position on Fig. 1) in the framework of the ICDP. Cores were collected using the GLAD800 drilling platform operated by the consortium for Drilling, Observation and Sampling of the Earth's Continental Crust (DOSECC). Site 2 was selected for multi-proxy high-resolution analyses by the PASADO science team because of higher core recovery (98.8%) and lower apparent sand content (Zolitschka et al., 2009). The sedimentary sequence at site 2 was built from 3 holes (Fig. 1; Kliem et al., 2013a,b) and has a composite length of 106.09 m.

3.2. Discrete samples

A series of 59 pilot cube samples ($2 \times 2 \times 2$ cm) were recovered from parallel cores (holes A, B and C at site 2; Fig. 1) at depths readily correlated to the composite profile using high-resolution core images. The cube samples were first used to measure the frequency dependence of magnetic susceptibility at room-temperature using Bartington dual frequency (0.46 and 4.6 kHz) MS2B meter. Difference in the susceptibility measured at low and high frequency is diagnostic of ultrafine (<0.03 μm) superparamagnetic and ferrimagnetic particles (Dearing, 1999). Afterward the anisotropy of magnetic susceptibility (AMS) was measured using the magnetic anisotropy susceptibility bridge "Roly-Poly" at the Institute for Rock Magnetism (IRM) of the University of Minnesota in Minneapolis. The best-fit AMS tensor was obtained by least-squares and the degree of AMS was calculated by dividing the maximum by minimum susceptibility.

The composite profile at site 2 was sampled at ca 40 cm intervals (total of 243 samples) for the measurement of hysteresis loops and derived properties including saturation remanence (Mr), saturation magnetization (Ms), bulk coercive force (Hc) as well as remanent coercive force (Hcr) using a Princeton Corp. alternating gradient force magnetometer (model MicroMag 2900 AGM). The magnetic properties Mr, Ms, Hc and Hcr depend on coercivity and domain state of the magnetic assemblage, and the ratios Mr/Ms and Hcr/Hc are commonly used as a magnetic grain size indicator (Day et al., 1977; Dunlop, 2002; Tauxe, 2010). The high-field magnetic susceptibility (k_{HF}) is the high-field slope of magnetization on the hysteresis curve. It reflects the contribution of non-ferrimagnetic material (diamagnetic and paramagnetic minerals), unsaturated antiferromagnetic minerals and unsaturated ultrafine superparamagnetic particles (e.g., Brachfeld, 2006). The proportion of high-field susceptibility for each sample was calculated by normalizing the hysteresis curve slope correction in a field of 0.3 T (k_{HF}) with Ms. As low coercivity minerals (magnetite and maghemite) are saturated in fields <0.3 T and higher coercivity minerals such as hematite and goethite are not (Dunlop and Özdemir, 2007), the proportion of high-field susceptibility reflect the hardness of the sediment in the absence of dia-, para- and superparamagnetic change. In order to further investigate the grain size distribution, 36 samples were selected for first-order reversal curve (FORC; Roberts et al., 2000) analyses in a saturating field of 1.2 T using the same instrument. Five of the discrete samples are associated to rock-magnetic facies 1 and were used for additional analysis. Unfortunately, no samples from facies 2 were left available. Magnetic extracts (using a neodymium hand-magnet) from rock-magnetic facies 1-*B*, *D*, *E*, *C* and *G* were analyzed using JEOL 6460LV scanning electron microscope equipped with an Energy Dispersive X-ray Spectrometer (SEM-EDS) in order to identify the iron minerals.

3.3. Continuous u-channel samples

The continuous u-channel samples from the composite sediment sequence at site 2 (99 sections; 106.09 m) were measured at 1-cm resolution. The natural, anhysteretic and isothermal remanent magnetizations (NRM, ARM, IRM) were measured using a minimum of 8 alternating field (AF) demagnetization steps (0, 10, 20, 30, 40, 50, 60 and 70 mT) using a 2G cryogenic magnetometer for u-channels. ARM was imparted with a peak AF of 0.1 T and a direct current (DC) bias field of 0.05 T. Susceptibility of anhysteretic remanent magnetization (kARM) was obtained by normalizing ARM by the DC field applied. Two IRMs at 0.3 T and 0.95 T were successively induced using a 2G pulse magnetizer and stepwise AF demagnetized. The low field magnetic susceptibility (k_{LF}) using a point sensor and the diffuse spectral reflectance (L^*, a^*, b^* color space) using a Minolta in-line spectrophotometer were measured on a GEOTEK Multi-Sensor Core Logger (MSCL) at 1 cm intervals at ISMER.

We use a set of rock-magnetic ratios and indicators to effectively discriminate between different magnetic minerals and magnetic grain sizes (e.g., Maher et al., 1999; Stoner and St-Onge, 2007). This approach is particularly useful when working with large datasets such as high-resolution measurements on continuous u-channel samples of long sediment cores. The median destructive field (MDF) is the field required to remove half of the initial remanence, whether natural or induced. It is influenced by magnetic grain size and mineralogy; hence MDF is a measure of the coercivity of a magnetic recording assemblage. Similarly, the remanence ratios permit isolation of a coercivity population between two demagnetization steps of a natural, anhysteretic or isothermal remanent magnetization (NRM, ARM or IRM). The ratio of ARM (or kARM) normalized by IRM is often referred to as the ARM ratio (e.g., Egli, 2004a; Lascu and Plank, 2013). It is commonly used as a magnetic grain size indicator for a magnetic assemblage dominated by magnetite because small single domain (SD) grains display disproportionately high ARM values (Maher and Taylor, 1988). As a result, the ARM ratio responds to small SD biogenic magnetite (Moskowitz et al., 1993; Snowball et al., 2002; Egli, 2004a) as well as to ultrafine magnetite near the superparamagnetic (SP)/stable singe domain (SSD) boundary, to SD extracellular or pedogenic magnetite particles (Özdemir and Banerjee, 1982; Maher and Taylor, 1988; Moskowitz et al., 1993; Frankel and Bazylinski, 2003; Maher et al., 2003; Egli, 2004a). The ratio of anhysteretic or

saturation isothermal remanent magnetization (ARM or SIRM) to magnetic susceptibility (k_{LF}) are also magnetic grain size indicators for a mineralogy dominated by magnetite (King et al., 1982; Thompson and Oldfield, 1986). SIRM/k_{LF} can be influenced by paramagnetic and superparamagnetic contributions (e.g., Thompson and Oldfield, 1986; Stoner et al., 1996) and for a magnetic mineralogy containing iron sulfides (greigite and pyrrhotite), high values of SIRM/k_{LF} are caused by typically low k_{LF} (Snowball and Thompson, 1990; Roberts, 1995; Fu et al., 2008). Higher values of SIRM/k_{LF} are associated with high coercivity minerals such as hematite and goethite because their strong resistance to magnetization results in relatively low IRM acquired in a given field than other magnetic minerals and exceptionally low k_{LF}, which is measured in a weak applied field (Maher, 2011). Finally, the ratio IRM/SIRM is useful to infer the degree of magnetic "hardness" i.e., the proportion of high coercivity minerals relative to low coercivity minerals (e.g., Stoner and St-Onge, 2007; Maher, 2011).

The sediment from Laguna Potrok Aike overall displays very high values of IRM in direct current (DC) fields of 0.3 T and 0.95 T (average value of all data >6 Am^{-1}; Table 1) and the intensity of $IRM_0$0.95 T is sometimes lower than $IRM_0$0.3 T. This is due to the inability of the cryogenic magnetometer system to accurately detect magnetization >ca 1 Am^{-1} in samples with high concentration of magnetic mineral (Roberts, 2006) such as the sediment from Laguna Potrok Aike (2–9 wt % of Fe_2O_3; Hahn et al., submitted for publication). This instrumental limitation obviously prevents us from using the IRM/SIRM ratio to track the relative contribution of high coercivity minerals in a continuous way; however the arithmetic average values for the different sediment types are included in Table 1. In this study, we use the remanence ratios, *k*ARM/$IRM_0$0.3 T (herein referred to the ARM ratio), $IRM_0$0.95 T/k_{LF} (herein referred to SIRM/k_{LF}) and $IRM_0$0.3 T/$IRM_0$0.95 T (herein referred to IRM/SIRM) from continuous u-channel samples data to identify rock-magnetic facies.

3.4. Lithology and chronology

Kliem et al. (2013a,b) described five lithological units for the composite sediment sequence from Laguna Potrok Aike based on the type of pelagic sediment and the frequency of MMDs. The simplified lithostratigraphic log as well as the radiocarbon-based chronology is presented in Fig. 2. The three lowermost units (10,609–8153 cm, 8153–4023 cm and 4023–1872 cm) correspond to the Last Glacial period and are characterized by progressive decrease in the percentage, frequency and thickness of MMD. From 1872 to 882 cm (Early Holocene, Lateglacial and ending Last Glacial) there is a dominance of pelagic laminated silts intercalated with thin fine sand and coarse silt layers, high content of plant macro remains and gastropods, few carbonate crystals and the occurrence of normally graded beds and pillow structures. The uppermost sediment type (882–0 cm) corresponds to the Holocene and consists of pelagic laminated silts with relatively high amounts of carbonates, in agreement with Nuttin et al. (2013). The chronology of the event-corrected composite depth (cd-ec) of the pelagic sediment sequence (4580 cm cd-ec) is based on a mixed-effect regression model of 58 radiocarbon dates and supported by 6 known tephra layers as well as by a global-scale magneto-stratigraphy using relative paleointensity (Kliem et al., 2013a; Lisé-Pronovost et al., 2013). Lithological and tephra correlation with previously studied cores from Laguna Potrok Aike further supports the radiocarbon-based chronology, including a core located nearby in the lake center covering the last 16,000 cal BP (PTA03/12-13; location on Fig. 1; Haberzettl et al., 2007) and a low-resolution core from a lake level terrace covering a similar time span (PTA03/5-6; location on Fig. 1; Haberzettl et al., 2009).

Table 1
Average values of selected parameters for rock-magnetic facies 1 and 2 compared to all data from Laguna Potrok Aike. Bold indicates notable data. The high values of SIRM/k_{LF} ($IRM_0$0.95 T/k_{LF}) in facies 1 is linked to low k_{LF} values. High values of ARM ratio (*k*ARM/$IRM_{0.3T}$) in facies 2 is linked to low $IRM_{0.3T}$ values.

	k_{LF} (10^{-5}SI)	NRM_0 (Am^{-1})	ARM_0 (Am^{-1})	IRM_0 0.3 T (Am^{-1})	IRM_0 0.9 T (Am^{-1})	IRM/ SIRM	ARM ratio (mmA^{-1})	SIRM/k_{LF} (kAm^{-1})
All data	137	0.033	0.18	6.5	6.2	1.08	0.78	7.4
Facies 1	**86**	0.027	0.14	6.3	5.9	1.07	0.65	**23.1**
Facies 2	117	0.025	0.17	**1.3**	1.5	0.88	**4.10**	2.6

4. Results

4.1. Magnetic assemblage

4.1.1. Discrete samples

The rock-magnetic analysis of cube samples reveals that 1) the degree of anisotropy is weak (less than 1.15), which indicates that the magnetic assemblage is not dominated by minerals with strong magnetocrystalline or shape anisotropy, and 2) the frequency-dependant magnetic susceptibility is generally lower than 2%, which indicates that there is no detectable superparamagnetic (SP) contribution (Dearing, 1999) in the general magnetic assemblage. Similar frequency-dependant results were obtained for the sediments of Laguna Potrok Aike for the last 16,000 cal BP (Gogorza et al., 2011, 2012), however we note that SP in low abundances are difficult to detect in the absence of low temperature measurements. The typical hysteresis curve for the pelagic sediment has a narrow loop and the shape is typical of pseudo single domain (PSD) magnetite (Fig. 4A) (Tauxe et al., 1996). The associated first-order reversal curve (FORC) diagram also indicates PSD magnetite with closed peak structures and coercivity spectra centered at ca 20 mT (Fig. 4A). The enlargement of the contours near the applied field axe (Hu) additionally indicates a possible contribution of MD or SP magnetite (Muxworthy and Roberts, 2007). The typical FORC diagram of tephra material displays a "kidney" shape towards higher coercivities (Fig. 4B). This shape is reported for iron sulfides greigite and pyrrhotite (Wehland et al., 2005; Roberts et al., 2006, 2011; Larrasoaña et al., 2007). The "kidney" shape is frequent in FORC diagrams of tephra material, in agreement with previous observation of iron sulfide framboids in the micropumice vesicles of reworked tephra from Laguna Potrok Aike (Jouve et al., 2013; Vuillemin et al., 2013). The "kidney" shape is also observed in different degrees in pelagic and MMD samples throughout the record, suggesting small contribution of iron sulfides in addition to magnetite. Together, cube and discrete sample analyses further support PSD magnetite as the dominant magnetic mineral in the sediment of Laguna Potrok Aike since 51,200 cal BP (Gogorza et al., 2011, 2012; Recasens et al., 2012; Lisé-Pronovost et al., 2013; submitted for publication).

4.1.2. Continuous u-channel samples

Fig. 4 presents a set of u-channel-based high-resolution magnetic properties for the PASADO sedimentary sequence (106.06 m). The average values of selected parameters are listed in Table 1. There is an overall low amplitude variability within the rock-magnetic parameters that is interrupted by peaks in the ARM ratio, SIRM/k_{LF}, Mr/Ms and k_{HF}/Ms. The peaks fall within or over MMD and represent two particular rock-magnetic signatures associated with two distinct types of gyroremanence best represented by remanence ratios NRM_{70}/NRM_0 (features *A* to *R*) and IRM_{40}0.3 T/

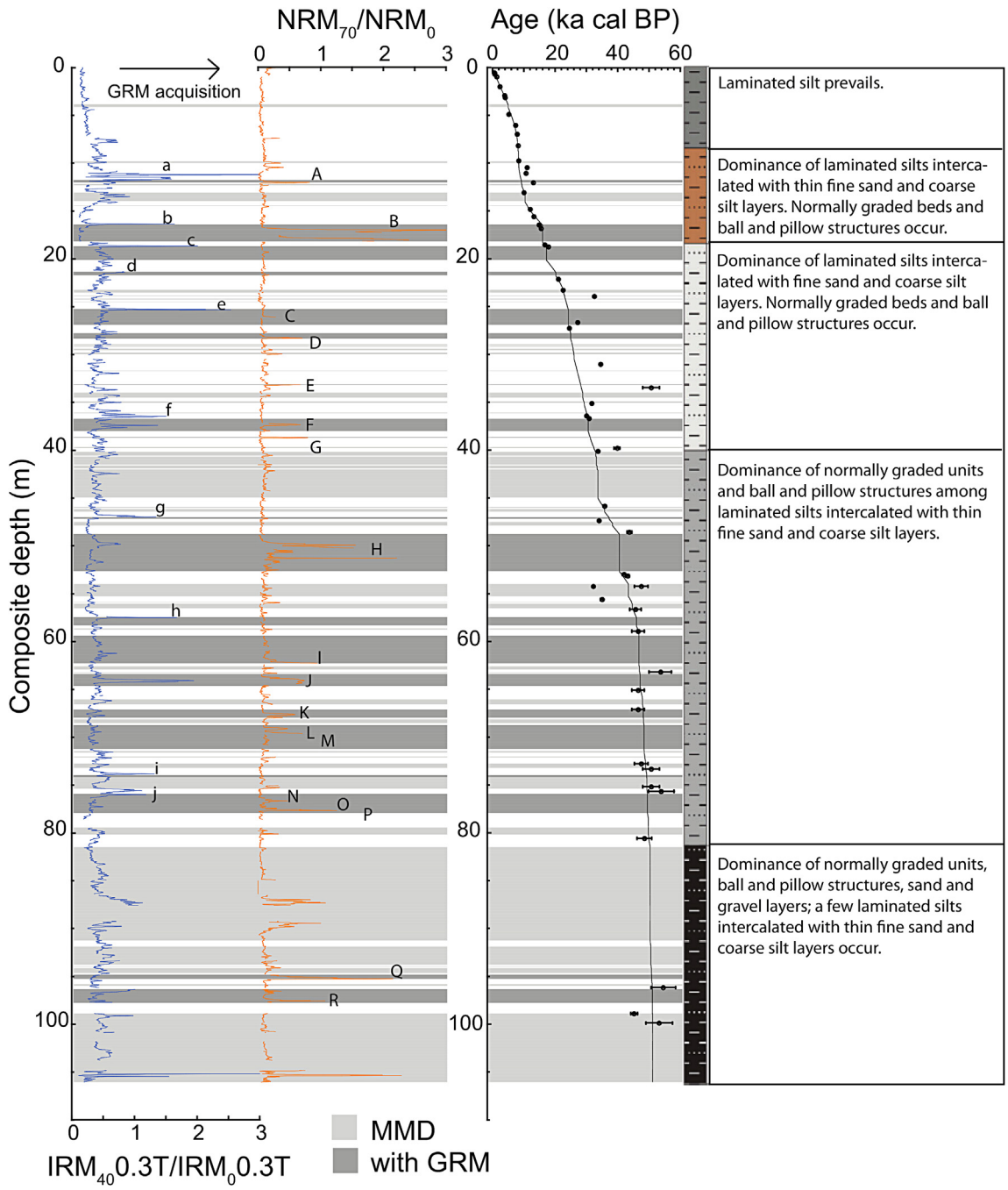

Fig. 2. Acquisition of gyroremanent magnetization (GRM) during static alternating field (AF) demagnetization of the sediment of Laguna Potrok Aike is observed within and over mass movement deposits (MMD; in light gray, those with GRM in dark gray). Rock-magnetic ratios $IRM_{40}0.3\ T/IRM_0 0.3\ T$ and NRM_{70}/NRM_0 indicate GRM acquired during AF demagnetization of isothermal and natural remanent magnetization, respectively. The lowercase and capital lettered features indicate the position of rock-magnetic facies 1 (from *A* to *R*) and rock-magnetic facies 2 (from *a* to *j*) discussed in the text. The radiocarbon-based chronology, lithological units and description from Kliem et al. (2013a,b) are presented on the right.

$IRM_0 0.3$ T (features *a* to *j*) associated to MMD (Fig. 2). These intervals are discussed in more detail.

4.2. Rock-magnetic facies

4.2.1. Facies 1

Rock -magnetic facies 1 represents 4.60 m or 4.3% of the total sediment record and is characterized by gyroremanence acquisition during AF demagnetization of the NRM, as indicated by high values of the remanence ratio NRM_{70}/NRM_0 (features *A* to *R*; Figs. 2 and 4). The spurious remanence is acquired perpendicular to the AF direction (Fig. 5) from 20 to 55 mT in sandy sediment and from 30 to 45 mT in tephra material. The example shown in Fig. 5 (facies 1E at 3316 cm) is composed of tephra material. Facies 1 is generally characterized by low and unstable NRM, low k_{LF} values, and peak values of $SIRM/k_{LF}$ (Table 1; Fig. 2). The discrete sample at 1732 cm depth is part of a reworked tephra displaying the facies 1 rock-magnetic properties (feature *B*; Fig. 2). Its FORC diagram displays

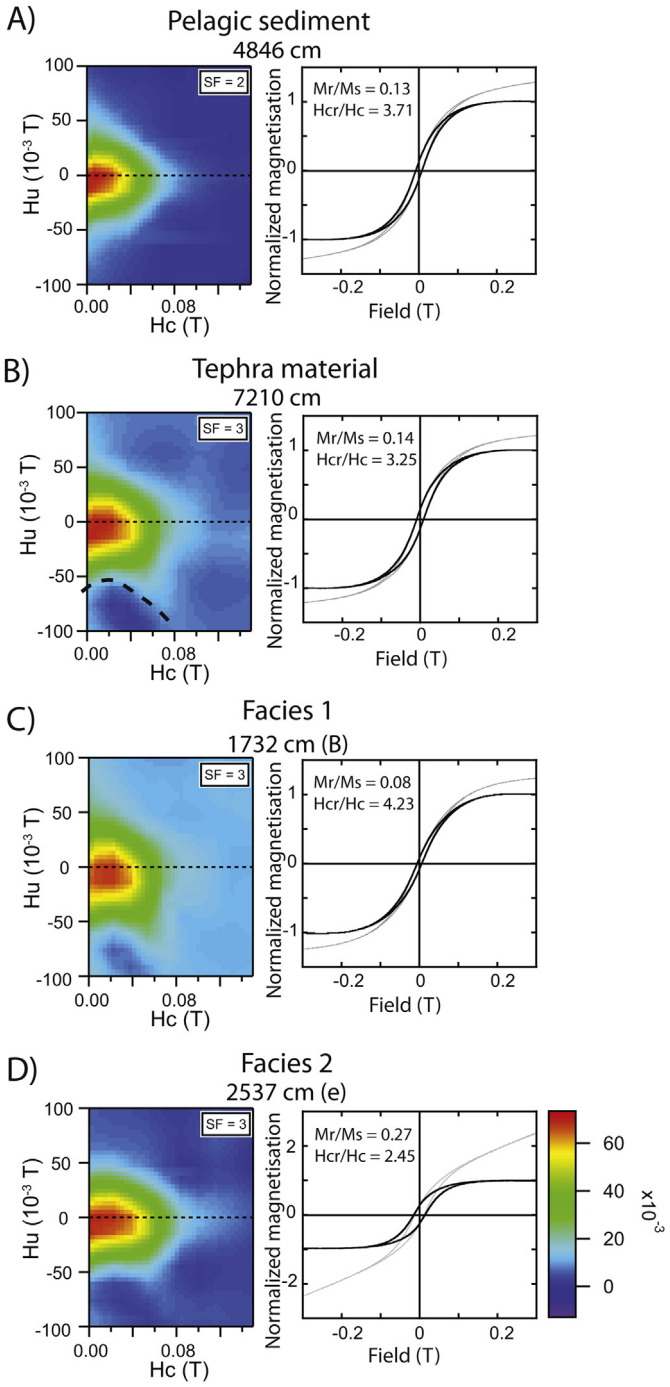

Fig. 3. First-order reversal curve (FORC) diagrams and hysteresis curves depicting the coercivity distribution of a typical pelagic sediment (A) and a tephra layer sample (B) from Laguna Potrok Aike, compared with samples from facies 1-*B* and 2-*e* (C and D). The raw (gray) and high-field slope corrected (black) magnetization are illustrated. The "kidney" shape indicated by a broken line on tephra's is reported for iron sulfides (Wehland et al., 2005; Roberts et al., 2011).

coercivity spectra centered at ca 20 mT and a "kidney" shape. The paleomagnetic directions display large amplitude changes in rock-magnetic facies 1, and in particular the paleomagnetic inclination sharply departs from the theoretical geocentric axial dipole (GAD) value for the site latitude (Fig. 6). Together the shape of the FORC diagram, gyroremanence during AF demagnetization of the NRM and peak values of SIRM/k_{LF} are diagnostic of iron sulfides such as greigite and pyrrhotite in facies 1 (Snowball, 1991; Roberts, 1995; Maher et al., 1999; Sagnotti and Winkler, 1999; Roberts et al., 2011). This is further supported by SEM-EDS identification of framboidal iron sulfides (Fe and S) in the facies 1 sample (Fig. 7). In addition, there are abundant iron oxide (Fe and O) coatings on all grain types (Fig. 7), as also observed in SEM-EDS analysis of thin slices (Jouve et al., submitted for publication).

4.2.2. Facies 2

Rock-magnetic facies 2 represents 0.99 m or 0.93% of the total sediment record and is characterized by maximum peak values of the ARM ratio (>2.5 mmA^{-1}), relatively lower IRM$_0$0.3 T values (Table 1; Fig. 4) and acquisition of gyroremanence during AF demagnetization of IRM. The latter is best represented by the remanence ratio IRM$_{40}$0.3 T/IRM$_0$0.3 T (Fig. 4). Acquisition of the spurious remanence between perpendicular and antiparallel to the alternating field begins between 5 and 15 mT and continues up to 15–35 mT, and then the sample is progressively demagnetized (Fig. 5). Paleomagnetic directions are stable and consistent with the GAD inclination for the coring site (Fig. 6) and there are sometimes single domain-like (SD) magnetic properties, as indicated by a higher Mr/Ms ratios (features *a*, *e*, *h*, *j*; Fig. 4) as well as MDF$_{ARM}$/MDF$_{IRM}$ values greater than 1 (*a*, *c*, *e*, *f*; not shown). The occasional SD-like properties and high values of the ARM ratio (average of 4.1 mmA^{-1}; Table 1) point to finer magnetic particles such as magnetosomes, authigenic magnetite and/or pedogenic magnetite (e.g., Moskowitz et al., 1993; Egli, 2004a). For magnetite, the high ARM ratio is attributed to the SD particle size, giving rise to unusually strong ARMs (Maher, 1988). However, in the sediment of Laguna Potrok Aike, peak values of the ARM ratio are not related to an ARM maximum, but to an IRM minimum (Table 1; Fig. 4). Therefore, and because not all intervals of facies type 2 display SD-like properties, finer magnetite particles alone cannot account for the magnetic signature and other magnetic minerals must be present.

The average IRM/SIRM values for facies 2 is lower than the average for the complete dataset and for the facies 1 (Table 1) pointing to a contribution of higher coercivity minerals. This is supported by a systematically lower proportion of saturation acquired in forward fields of 0.3 T and 0.95 T (Table 1; Fig. 4), and by higher values of high-field susceptibility (Fig. 4). For instance, the sample at 2537 cm cd (corresponding to feature *e* of facies 2) has a steeper high field slope in the raw hysteresis loop (Fig. 3, light gray curve) relative to the typical pelagic, fine sediment, and tephra material. Because there is no significant dilution of the concentration-dependant rock-magnetic properties in facies 2 (Fig. 4) as would be expected for an increase in para- or diamagnetic contributions, the steep slopes are attributed to unsaturated magnetic minerals in a 0.3 T field, and could additionally reflect a contribution of ultrafine superparamagnetic particles. Finally, the more open hysteresis loop and a FORC diagram covering a slightly larger range of coercivities than the typical pelagic sediment (Fig. 3) is also consistent with a contribution of high coercivity minerals such as hematite and goethite to facies 2.

4.2.3. Stratigraphy of the rock-magnetic facies

Rock-magnetic results reveal that the higher proportion of magnetic minerals besides magnetite is found in relation to MMDs in the sediment of Laguna Potrok Aike. Iron sulfides (facies 1) are found within MMDs composed of sands and tephra (Fig. 6), and high coercivity minerals (facies 2) are found in sediment deposited immediately above MMDs (for example the features *i* and *j*; Fig. 6). Weaker rock-magnetic signatures in facies 2 occur within MMDs, but with lower intensity (e.g., ARM ratio < 2.5 mmA^{-1}). We now focus on the 10 strongest signatures denoted as *a* to *j* (Figs. 2 and 4).

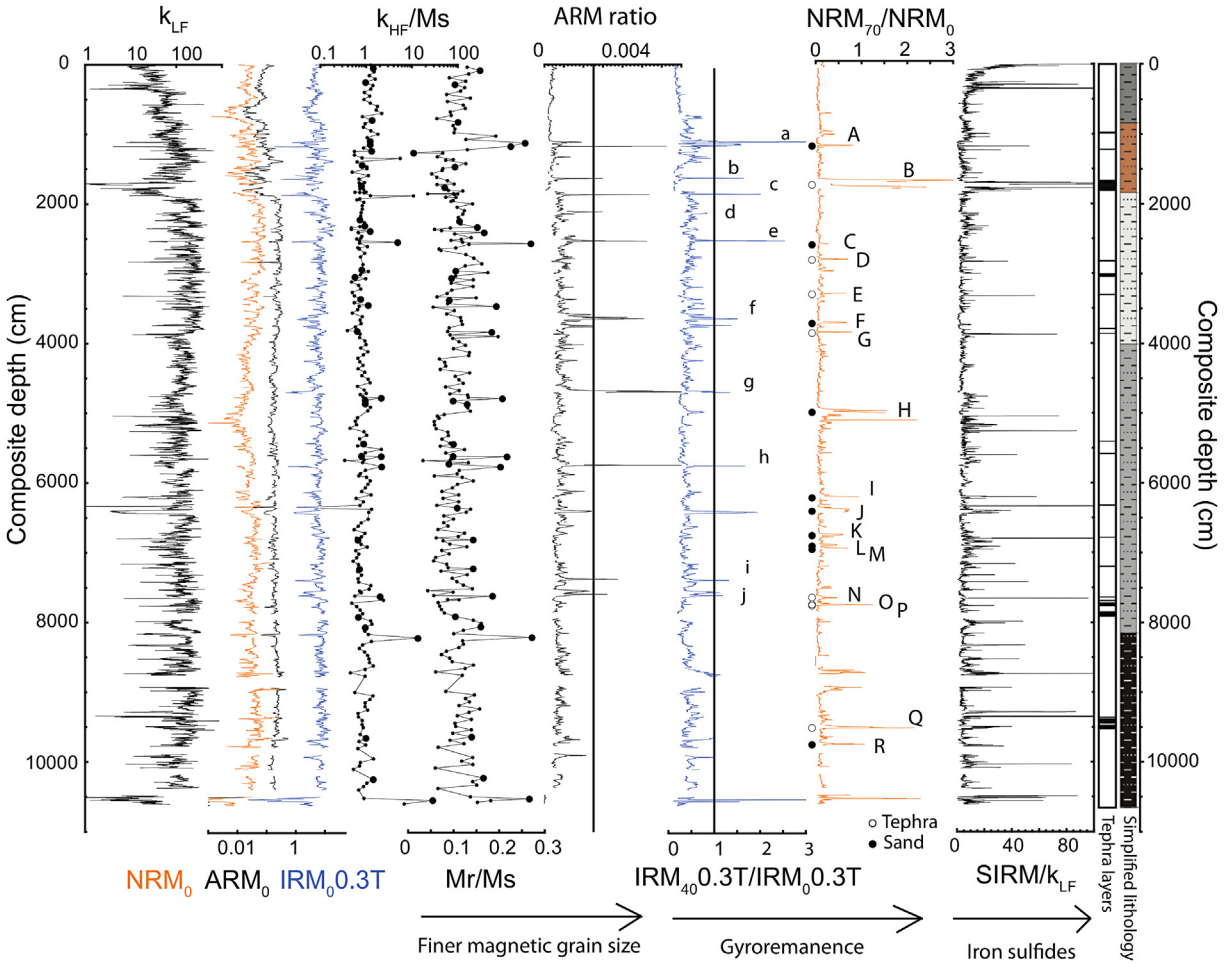

Fig. 4. Rock-magnetic properties of the composite sedimentary sequence at site 2 from Laguna Potrok Aike. From left to right: low field magnetic susceptibility (k_{LF}), natural (NRM_0), anhysteretic (ARM_0) and isothermal ($IRM_0$0.3 T) remanent magnetizations before alternating field (AF) demagnetization, and the proportion of high-field susceptibility normalized by saturation magnetization (k_{HF}/Ms) are presented on a log scale. The grain size indicators Mr/Ms and the ARM ratio (kARM/$IRM_0$0.3 T) are presented. Selected samples for FORC analyses are shown with larger symbols on k_{HF}/Ms and Mr/Ms curves. High values of the remanence ratio IRM_{40}0.3 T/$IRM_0$0.3 T that indicate the acquisition of gyroremanence during AF demagnetization of IRM within rock-magnetic facies 2 is labeled from *a* to *j*. High values of the remanence ratio NRM_{70}/NRM_0 that indicate gyroremanence acquisition during AF demagnetization of NRM within rock-magnetic facies 1 is labeled from *A* to *R*. Symbols (open or closed) represent the associated sediment type (tephra or sand, respectively) of type 1 intervals. Peak values of SIRM/k_{LF} ($IRM_0$0.95 T/k_{LF}) are indicative of iron sulfides (Maher et al., 1999). The position of tephra layers and lithological units from Kliem et al. (2013a,b) are presented on the right panel.

The L^* values is a useful indicator of (white-colored) tephra layers, which are sometimes associated with iron sulfides at Laguna Potrok Aike (e.g., features *O* and *P*; Fig. 6). While not all sand- and tephra-bearing MMD have rock-magnetic signatures of facies 1, iron sulfides (facies 1) are most frequently located directly at the base of MMD horizons, and a series of facies 1 features are sometimes observed within a MMD (for example features *N*, *O* and *P* in MMD52; Fig. 6). Four MMDs are associated with both facies (1 and 2). However, most of the time the facies occur independently of each other, suggesting there is no link between their formations. Visual description of the rock-magnetic facies 2 sediment and associated MMDs are presented in Table 2. There is often plant macro remains of aquatic mosses visible in the sediment and the MMDs are either capped with sands, reworked tephra material (feature *b* is located above a tephra from Reclus volcano; Wastegård et al., 2013) or a gray mud layer. Feature *a* is the only one displaying yellow coloration. Interestingly, three gray mud layers (associated to features *c*, *h* and *j*) visibly overlay sediment containing clay aggregates (Fig. 8) recently interpreted as indicators of permafrost melt (Jouve et al., submitted for publication). In summary, facies 1 is characterized by iron sulfides inside MMDs composed of sand and tephra material, whereas facies 2 is characterized by high coercivity minerals deposited on the top of MMDs of various compositions.

5. Discussion

5.1. Gyroremanent magnetization (GRM) and magnetic mineralogies

While the GRM acquisition during AF demagnetization of the NRM (such as in facies 1) is frequently used as diagnostic of iron sulfides in sediments (Snowball, 1997; Hu et al., 1998, 2002; Stephenson and Snowball, 2001; Roberts et al., 2011), to our knowledge the acquisition of GRM during AF demagnetization of the IRM (such as facies 2) was not previously reported. We interpret the acquisition of GRM in the facies 2 as indicative of field-dependant anisotropy in hematite and/or goethite particles. From Stephenson (1980), it is well known that the anisotropy of a sample is responsible for the GRM acquisition during AF demagnetization. Consequently, only a magnetic mineral becoming magnetically anisotropic when subjected to an IRM can account for the acquisition of GRM *uniquely* during AF demagnetization of the IRM (and

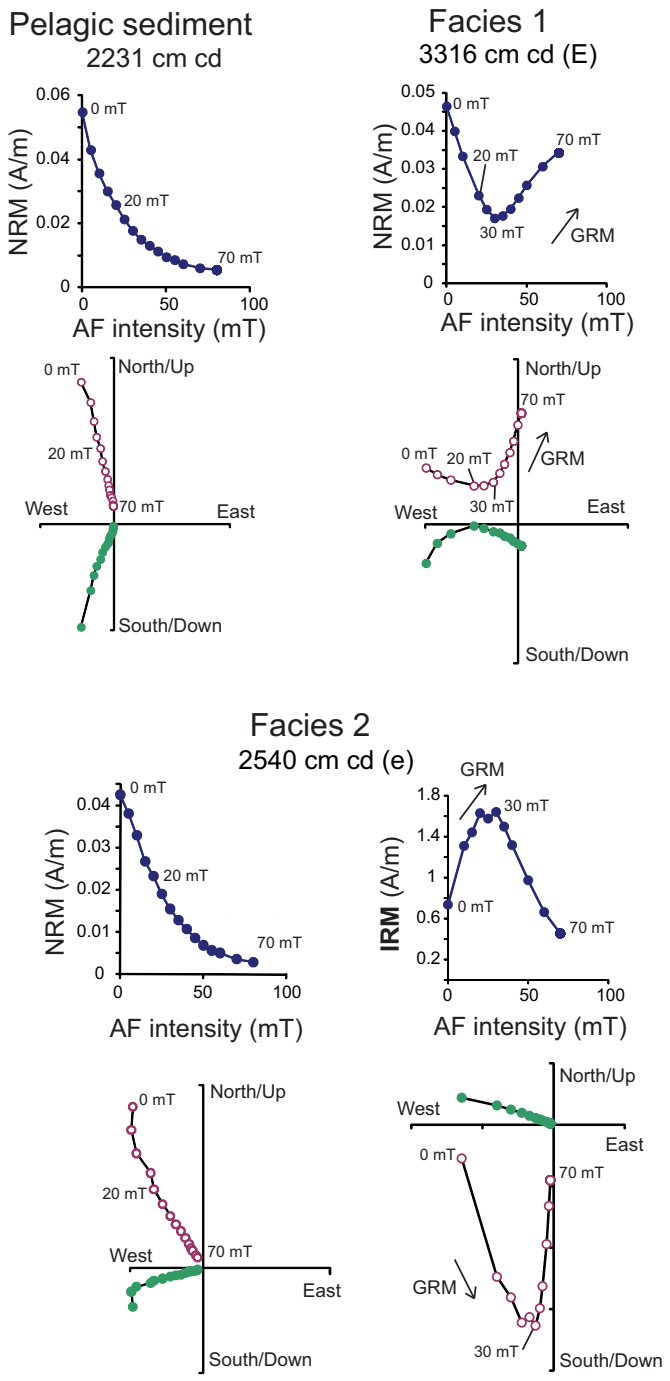

Fig. 5. Demagnetization plots and orthogonal projection diagrams illustrating the typical behavior of pelagic sediment from Laguna Potrok Aike, facies 1 and 2. Arrows indicate the spurious gyroremanent magnetization (GRM) acquired during AF demagnetization of NRM (facies 1) and IRM (facies 2). Open (closed) symbols in the vector end-point orthogonal diagram represent projection in the vertical (horizontal) plane.

not during AF demagnetization of the NRM and ARM; Fig. 5). Moreover, the fact that intervals displaying GRM during AF demagnetization of IRM also display contrasting rock-magnetic signature (facies 2) reveals that technical malfunction such as transient deformation of the AF waveform (Roperch and Taylor, 1986) is rather unlikely as this particular magnetic behavior is not seen elsewhere in the record.

Both hematite and goethite minerals have crystal asymmetry due to structural defects and/or substitutions and as a result, display variable rock-magnetic properties (Dekkers, 1989; Rochette et al., 2005; Liu et al., 2010). The acquisition of GRM in facies 2 could be linked to a metastable domain state of pedogenic hematite as was hypothesized by Tauxe et al. (1990). This interpretation is supported by a simple model of realistic acicular SD particles by Potter and Stephenson (2006) revealing that hematite particles can display a range of variable stable orientations resulting in large field-impressed anisotropy and GRM acquisition during alternating field demagnetization. The distinctive contribution of high coercivity minerals in rock-magnetic facies 2 (and the absence of iron sulfides such as greigite and pyrrhotite) hence suggests that pedogenic hematite and/or goethite could account for the observed GRM acquisition. In addition, a near anti-parallel orientation of the GRM in some of the facies 2 might also indicate grains prone to self-reversal as reported for oxidized iron oxides such as maghemite and ilmeno-hematite (Channell and Xuan, 2009; Roperch et al., 2012). If this is the case, the GRM acquired during AF demagnetization of the NRM and ARM must have been swamped by the strong normal component held by detrital magnetite and only detectable during AF demagnetization of the IRM because of field-impressed anisotropy.

5.2. Origin of magnetic minerals

5.2.1. Authigenic formation of iron sulfides in facies 1

The production of magnetic iron sulfides such as greigite and pyrrhotite in sediments requires sulfate-reducing conditions (Konhauser, 1998; Sagnotti, 2007). Early diagenetic pyrrhotite is unlikely to form at temperatures <180 °C (Horng and Roberts, 2006), however greigite is commonly preserved in marine or lacustrine sediment when the pyritization process is interrupted (e.g., Fu et al., 2008; Blanchet et al., 2009; Brachfeld et al., 2009) by decomposable organic matter, dissolved sulfate and/or reactive iron limitation (Berner, 1984). While there are abundant iron oxides in Laguna Potrok Aike (Gogorza et al., 2012; Lisé-Pronovost et al., 2013; submitted for publication), the very low organic matter content in the sediment (average of 0.55% and 0.98% during the Last Glacial period and since 17,300 cal BP, respectively; Hahn et al., 2013) and the variable amount of dissolved sulfate (from 0 to 1500 ppm; Vuillemin et al., 2013) most likely limited pyritization. The low k_{LF} values of facies 1 (Table 1), the weak and unstable NRM as well as the sharp inclination change (Fig. 6) altogether point to dissolution of detrital magnetite, which in turn would have provided the required reactive Fe^{2+} for iron sulfides formation.

We infer that while diffusing upward, the Fe^{2+} reacted with available organic matter and dissolved sulfate in the pore water to form greigite. It is unclear whether organic matter or sulfates limited pyritization in tephra layers. Nevertheless, precipitation of iron oxide coatings on minerogenic grains indicate excess Fe^{2+} reaching the oxic/anoxic boundary (Stumm and Morgan, 1996; Gobeil et al., 1997). The situation is different in sand layers, where abundant pore water sulfate suggests that organic matter most likely limited the process of pyritization. A low-resolution study of site 1 (position on Fig. 1) (Vuillemin et al., 2013) identified three intervals of significantly higher pore water sulfate interpreted as major mafic inputs to the lake. The depth correlation between sites 1 and 2 (Gehbardt, pers. comm.) indicates that these mafic inputs correspond to the cluster of facies 1 features *-I* to *-M*, and features 1-*H* and *-F* in reworked sand layers at site 2 (Fig. 4). Hence, preservation of greigite in these mafic sand layers was most likely promoted by higher sulfate availability and limited by low organic matter content. The high-resolution rock-magnetic identification of greigite in facies 1 provides support to the interpretation of

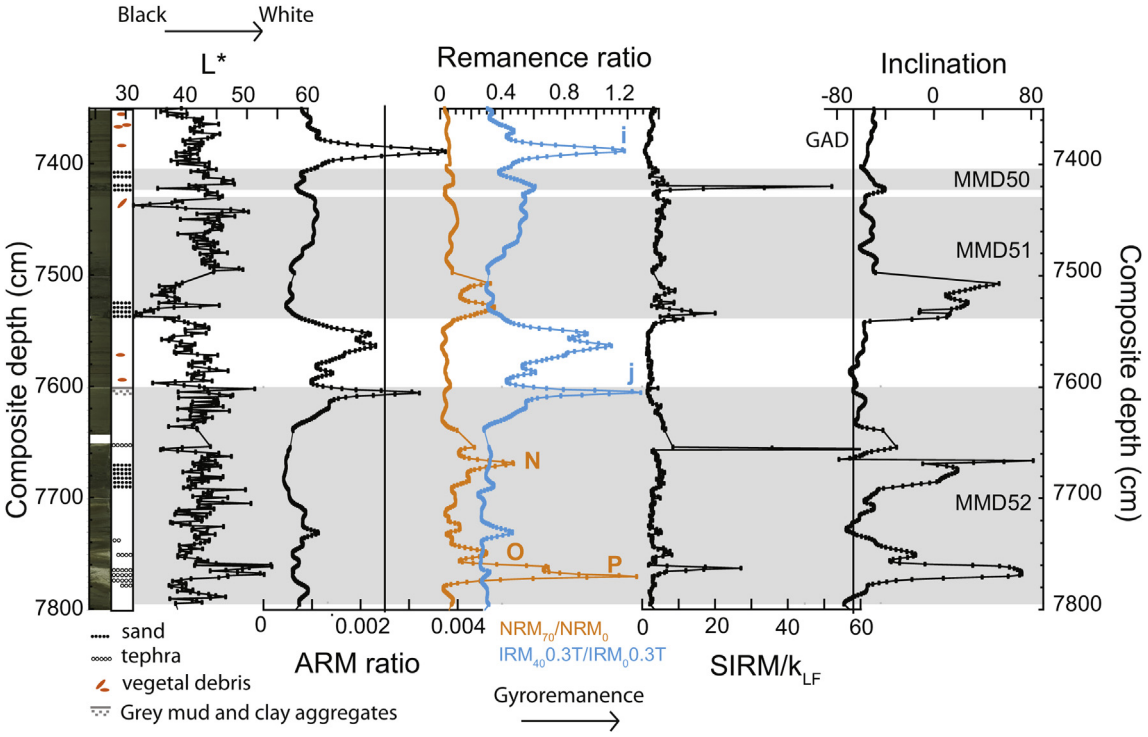

Fig. 6. Stratigraphy of facies 1 and 2 with mass movement deposits (MMDs) in the interval 73–78 m blf. From left to right: core photograph, and simplified lithostratigraphic log, L^*, ARM ratio (ARM/$IRM_0$0.3 T), remanence ratios IRM_{40}0.3 T/$IRM_0$0.3 T and NRM_{70}/NRM_0, SIRM/k_{LF} and paleomagnetic inclination. The vertical line on the inclination plot indicates the theoretical value for a geocentric axial dipole (GAD) at the latitude of the coring site. The MMDs are underlined in gray and the features *N*, *O*, *P* (facies 1) as well as *i*, *j* (facies 2) are indicated.

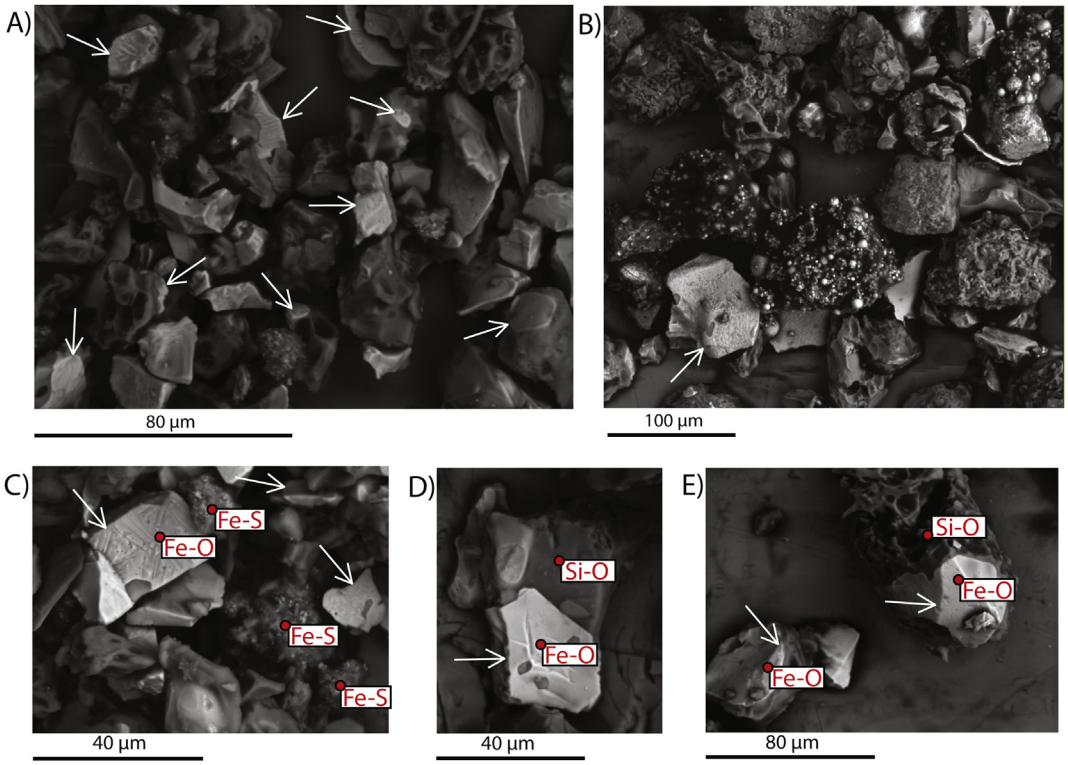

Fig. 7. Scanning electron microscopic (SEM) images and X-ray identification of framboidal iron sulfides and iron oxide coatings in facies 1. Red circles indicate spots for X-ray element analyses and white arrows indicate iron oxide coatings precipitated on detrital grains. A) General view of iron oxide coatings on various types of detrital grains in facies1-*G*, B) aggregates of framboidal iron sulfides and iron coating in facies 1-*B* and C) in facies 1-*D*, close-up of D) iron oxide coating on a detrital grains in facies 1-*E* and E) on micropumice in facies 1-*G*. (For interpretation of the references to color in this figure legend, the reader is referred to the web version of this article.)

Table 2
Description of the sediment and mass movement deposits (MMDs) associated with the 10 labeled rock-magnetic facies 2.

Rock-magnetic facies 2		Depth[a] (cm cd)	Age[a] (cal BP)	Mass movement deposit	
Name	Sediment description			Thickness (cm)	Sediment description
a	Yellow color; vegetal debris	1184	9260 ± 715	22	Sands
b	Layer of vegetal debris	1648	16030 ± 560	174	Reworked tephra material including mud laminations
c	Gray mud overlaying clay balls in the MMD	1875	17320 ± 543	141	Mud
d	Layer of vegetal debris	2143	20250 ± 672	34	Sand at base, fining upward with plant debris on top
e	Gray mud	2533	24280 ± 1140	158	Mud
f	Mud	3678	30640 ± 1313	126	Mud and sands
g	Mud	4708	37290 ± 1316	12	Sand layers with mud clasts
h	Gray mud overlaying clay balls in the MMD	5753	46000 ± 4484	82	Sand at base, fining upward
i	Laminated mud	7403	49320 ± 7790	20	Sand and mud
j	Gray mud overlaying clay balls in the MMD	7600	49580 ± 8077	202	Mud, sand and tephra material, folded structure

[a] Depth and age as on the top of the MMD.

Vuillemin et al. (2013) and additionally reveals 3 previously undetected sand layers with the same rock-magnetic signature (facies 1 features -*A*, *C*, and *R*). Despite minimal diagenetic processes in the sediment of Laguna Potrok Aike (Nuttin et al., 2013; Vuillemin et al., 2013; Hahn et al., submitted for publication), our results reveal that adequate conditions for the authigenic formation of greigite were reached in some MMDs.

5.2.2. *Input of pedogenic particles for facies 2*

Rock-magnetic data reveal a series of 10 short intervals (facies 2) with a magnetically significant proportion of high coercivity minerals (hematite and/or goethite). We interpret these intervals as containing pedogenic particles transferred to the lake by extreme runoff events based on geological, limnological, stratigraphic and climatic evidences.

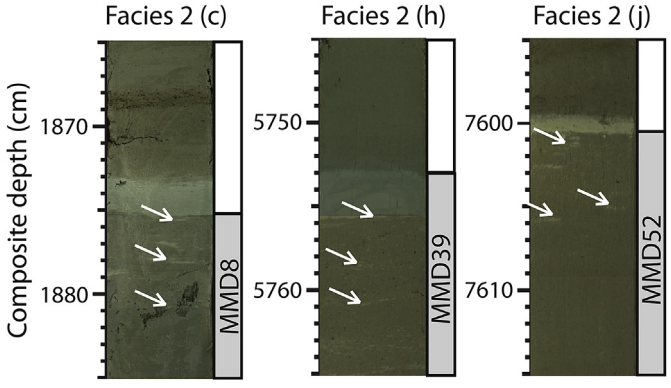

Fig. 8. Core photograph showing clay aggregates (some are pointed using white arrows) and mass movement deposits (MMDs) associated to facies 2 features *c*, *h* and *j*.

First, we consider the possible sources of high coercivity authigenic or detrital minerals in lake sediments. There is no paleolimnological evidence (since 51,200 cal BP; Zolitschka et al., 2013, 2009) that Laguna Potrok Aike met the hypersaline and acidic lake conditions required for precipitation of authigenic hematite concretions, as documented for Lake Brown (Australia) and possibly also for planet Mars (Bowen et al., 2008), or for the precipitation of authigenic goethite as reported in acidic mining lakes (Blodau and Gatzek, 2006). Additionally, the slow process of in-situ iron oxide oxidation at the sediment/water interface (e.g., Robinson, 2000) is unlikely for Laguna Potrok Aike because of high sedimentation rates (average of 90 cm/ka; Kliem et al., 2013a,b). Stable magnetic grain size and concentration-dependant parameters (e.g., MDF_{NRM}, ARM) as well as the maintained stability of the NRM in facies 2 argue against diagenetic alteration of magnetic minerals. Therefore, the high coercivity minerals in facies 2 are interpreted as a detrital addition to the magnetic assemblage. Moreover, as there are no hematite or goethite-bearing rocks in the Pali Aike volcanic field (Ross et al., 2011; Coronato et al., 2013), the most likely source is through oxidation of the abundant detrital magnetite in the lake catchment. The iron oxides maghemite, hematite and goethite are typically associated with soils and paleosols

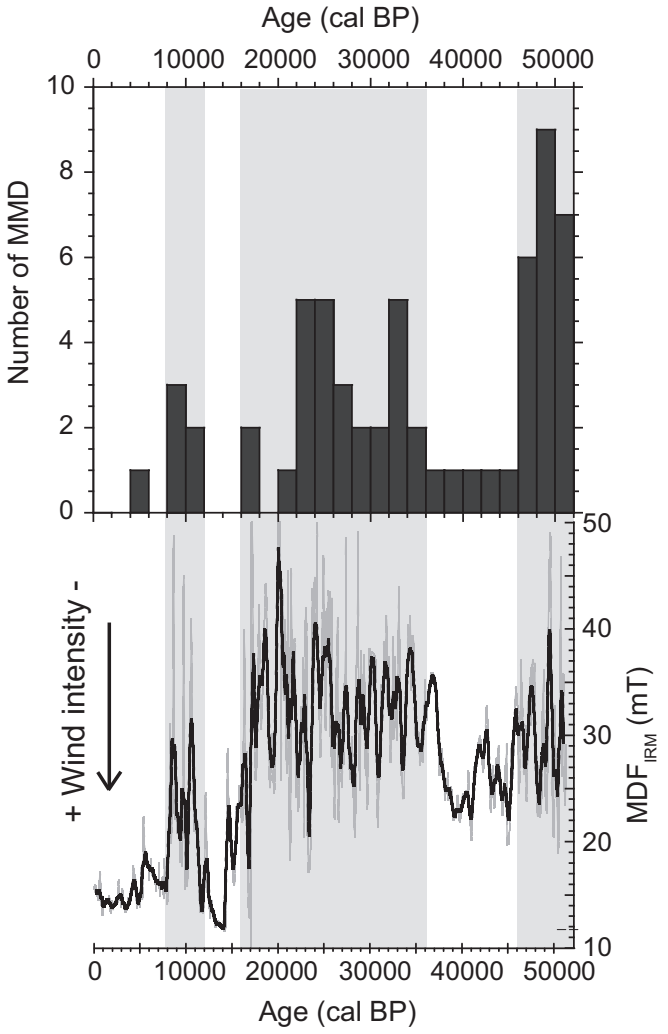

Fig. 9. Comparison of the frequency of mass movement deposits (MMDs) per 2000 years intervals and wind intensity proxy from Laguna Potrok Aike (MDF_{IRM}; Lisé-Pronovost et al., submitted for publication).

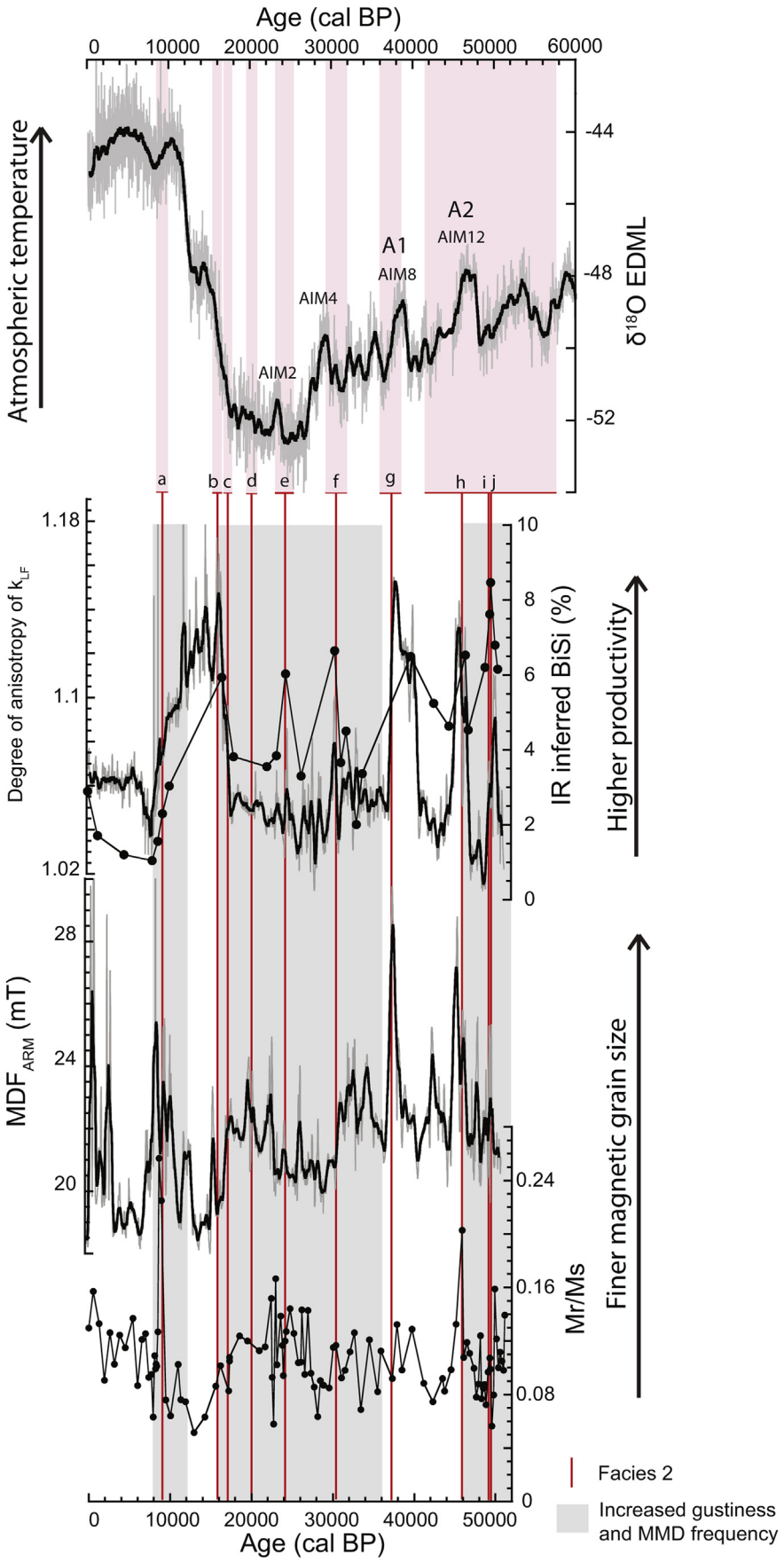
Age (cal BP)
0
10000
20000
30000
40000
50000
60000
Atmospheric temperature
-44
-48
-52
δ18O EDML
A2
AIM12
A1
AIM8
AIM4
AIM2
a
b c
d
e
f
g
h
i j
1.18
1.1
1.02
Degree of anisotropy of kLF
10
8
6
4
2
0
IR inferred BiSi (%)
Higher productivity
28
24
20
MDFARM (mT)
0.24
0.16
0.08
0
Mr/Ms
Finer magnetic grain size
Facies 2
Increased gustiness and MMD frequency
Age (cal BP)

(Dunlop and Özdemir, 2007; Maher, 2011). Maghemite (γFe_2O_3) is a cation-deficient spinel formed during pedogenesis, and is difficult to distinguish from magnetite based solely on room-temperature rock-magnetic properties. Further oxidation leads to hematite and goethite, which are "hard" antiferromagnetic minerals (e.g., Maher et al., 1999). Soil formation in arid to semi-arid climates strongly depends on precipitations. In particular, when the mean annual precipitation is lower than ca 200 mm/yr, bacterial activity (which releases the Fe^{2+} for pedogenic magnetite precipitation) becomes limited, and as a result hematite and goethite accumulate (Maher, 2011). We note that goethite is more ubiquitous in soils than hematite, which is typically associated to tropical and sub-tropical climate (e.g., Maher, 2011). However, well-drained soils in a cooler climate can result in preferential accumulation of hematite when short periods of wetness alternate with long warm and dry periods (Schwertmann et al., 1982; Maher, 1998) and hematite was reported for Argentinean loess using rock magnetic, Mössbauer spectroscopy, and bulk geochemical measurements (Carter-Stiglitz et al., 2006). Regardless of the precise magnetic mineralogy, the high coercivity contribution in the PASADO record is interpreted as resulting from oxidation of detrital magnetite and the occasional SD-like properties of facies 2 possibly indicate a variable proportion of SP/SD magnetite and maghemite precipitated during wetter periods. In a biplot of MDF_{ARM} vs ARM ratio designed to identify the provenance of magnetite particles (Egli, 2004a), rock-magnetic facies 2 clusters in a region between pedogenic/extracellular and biogenic magnetite (Supplementary data). This further supports the presence of pedogenic particles in facies 2 and reveals a possible contribution of biogenic magnetite.

Second, we discuss the possible transport processes of pedogenic particles to the lake. Extreme precipitation events, snowfall and permafrost melt could generate runoff capable of carving gullies and canyons such as those visible around the lake (Fig. 1). Sudden water input can generate instabilities on the steep lake slopes and trigger a MMD above which the very fine pedogenic particles would settle. Today, extreme precipitation events are documented uniquely at times of weak SWW, when easterly and northern winds reach the region (Ohlendorf et al., 2013; Schäbitz et al., 2013) (Fig. 1B). Fig. 9 suggests that this relationship was probably maintained in the past for times of weaker winds (Lisé-Pronovost et al., submitted for publication) associated with higher MMD frequency in Laguna Potrok Aike since 51,200 cal BP (Kliem et al., 2013a,b). This interpretation builds on the idea of "event resistance" where in the presence of consistently strong winds from the same direction (e.g., the SWW during the Holocene), all the sediment able to be moved is moved after a certain period of time. As a result the number of MMD horizons decreases or cease, and there is a need for wind direction change and/or more extreme events to trigger the next MMD (Eden and Page, 1998). This is illustrated by absence of facies 2 in the PASADO record since the onset of strong SWW (Zolitschka et al., 2013; Lisé-Pronovost et al., submitted for publication). In contrast, without persistent SWW over Laguna Potrok Aike during the Last Glacial period (Zolitschka et al., 2013; Hahn et al., submitted for publication; Lisé-Pronovost et al., submitted for publication), frequently changing wind directions and intensities (increased gustiness) could account for more frequent MMDs. This mechanism explains facies 2 and its relation to MMDs in the PASADO record. In addition, the presence of more humid air masses from the Atlantic could have favored soil formation through more frequent precipitation and contribute to higher lake levels during the Last Glacial (Zolitschka et al., 2013). Interestingly, periods of simultaneous slides in Laguna Potrok Aike at 7800 cal BP and 4900 cal BP were identified using seismic surveys (Anselmetti et al., 2009) and correspond to the two latest periods of increased MMD frequency and relatively lower wind intensities (Fig. 9). Our results thus hint at greater gustiness as probable cause for these events, in addition to seismic shaking as hypothesized by Anselmetti et al. (2009). Finally, the timing of rock-magnetic facies 2 further supports the proposed transport mechanism because all pedogenic runoff events occur during times of higher MMD frequency and gustiness (gray highlight on Fig. 10).

5.3. Paleoclimatic implications

The formation of authigenic iron sulfides in the PASADO record indicate reducing conditions inside some MMD horizons. The reworked mafic sands of facies 1 were likely supplied from mafic rocks located on the south-west lake shore and could indicate increased erosion in this area by wave action and/or the temporary activation of a paleochannel visible on Fig. 1 during a runoff event. Facies 1 features in reworked tephra material has no clear paleoclimatic implications. In contrast, in facies 2 the transport and deposition of pedogenic particles via runoff is necessarily climate-driven.

Events *g* and *h* (Table 2) correspond (within limits) to the two warmer periods of the Last Glacial as recorded in Antarctica (A1 and A2, Blunier and Brook, 2001; AIM8 and AIM12, EPICA community members, 2006). These Antarctic warm periods also associated to higher atmospheric CO_2 concentrations and lower dust fluxes to Antarctica (EPICA community members, 2006) are characterized elsewhere in the Southern Hemisphere by increased sea-surface temperature (Barrows et al., 2007; Caniupán et al., 2011) and increased wind-driven upwelling in the Southern Ocean (Anderson et al., 2009), suggesting significant large-scale reorganization of the atmosphere-ocean system. In Laguna Potrok Aike, these periods correspond to increased productivity (Hahn et al., 2013) and to finer magnetite grains, as indicated by rock-magnetic properties which are sensitive to smaller grains (MDF_{ARM} and Mr/Ms) (Fig. 10). Finer magnetite grains during warmer and more productive periods could indicate bacterial magnetite (Egli, 2004b). Interestingly, the degree of anisotropy of the magnetic susceptibility (although at only very low resolution) appears to follow changes in lake productivity and hence supports the presence of anisotropic biogenic magnetosomes typically occurring in chains (Moskowitz et al., 1993; Snowball et al., 2002). Event *h* likely associated with A2 (at 46,000 cal BP; Table 2) is one of the three runoff events that corresponds to clay aggregates in the sediment (Fig. 8). Building on the recent micro-sedimentological study of Jouve et al. (submitted for publication), we interpret clay aggregates as direct evidence of melting permafrost bringing pedogenic iron minerals locked or formed within permafrost (e.g., Vogt and Larqué, 2002) to the lake. Relict sand wedges attest to the presence of permafrost near Laguna Potrok Aike in the past (Bockheim et al., 2009) and Kliem et al. (2013b) recently dated a sand wedge from the Last Glacial

Fig. 10. Comparison of the paleotemperature proxy ($\delta^{18}O$) from Antarctica (EPICA community members, 2006), Laguna Potrok Aike productivity proxy (biogenic silica: BiSi; Hahn et al., 2013) and rock-magnetic properties including the degree of anisotropy of magnetic susceptibility, the median destructive field of anhysteretic remanent magnetization (MDF_{ARM}), and the ratio Mr/Ms. MDF_{ARM} and Mr/Ms indicate changes in the smaller magnetic grain size fraction and are especially sensitive to SD magnetite (Maher, 1998; Dunlop and Özdemir, 2007). Thick black curves represent the millennial-scale variability and gray curves high-resolution data. The shading indicates periods with higher MMD frequency, generally lower wind intensity and increased gustiness (cf. Fig. 8.). Red vertical lines indicate the timing of pedogenic minerals in the sediment record of Laguna Potrok Aike (facies 2 from *a* to *j*) and pink lines represent the age uncertainty of the radiocarbon-based chronology (Kliem et al., 2013a,b). Antarctic isotope maximum (AIM; EPICA community members, 2006) and Antarctic warm events A1 and A2 (Blunier and Brook, 2001) are indicated. (For interpretation of the references to color in this figure legend, the reader is referred to the web version of this article.)

period near Laguna Potrok Aike using optically stimulated luminescence (OSL) dating.

The two other periods of higher lacustrine productivity in Laguna Potrok Aike are at ca 50,000 cal BP and from the deglaciation to the Early Holocene (Hahn et al., 2013). Both are associated with input of pedogenic minerals (facies 2). The event *j* corresponds to clay aggregates in the sediment (Fig. 8) interpreted as permafrost melt. The closely following event *i* most likely results from a precipitation event because it is not associated with clay aggregates and overlays a MMD of muddy sands with plant macro remains of aquatic mosses suggesting erosive action at lower depths. The age uncertainty of the radiocarbon-based chronology is large in the older part of the record, but the events *i*, *j* and the coeval maximum productivity could correspond to the warming at ca 54,000 cal BP recorded in Antarctica (EPICA community members, 2006) (Table 2; Fig. 10). Alternatively, the lake productivity could have been triggered by the input of nutrients by runoff and sediment remobilization as also hypothesized by Hahn et al. (2013). Events *b* and *c* correspond to the onset of deglaciation in the mid-latitudes of the Southern Hemisphere (17.3 ka cal BP; Schaefer, 2006) and to two sudden rise in temperature in southern South America (McCulloch et al., 2000). Event *c* at 17,320 cal BP corresponds (within the limit of the chronology) to the end of a major glacier advance of the southern Patagonian Ice Sheet (PIS) in the Magellanes Strait (Sugden et al., 2009) and to the retreat of the Seno Skyring Glacier (Kilian et al., 2007) only ca 100 km south-west of Laguna Potrok Aike. It is also the youngest event characterized by clay aggregates (Fig. 8) and interpreted as the result of permafrost melt. The following event *b* at 16,030 cal BP is interpreted as linked to extreme precipitation event(s) because it overlays a thick MMD (174 cm) composed of tephra material including mud laminations and layers of plant macro remains. Finally, the more recent event (*a* at 9260 cal BP; Table 2) is also associated with high lacustrine productivity and fine magnetite grains (Fig. 10) and the yellow coloration (Table 2) of the sediment supports the presence of goethite for this interval (Schwertmann, 2008). Runoff event *a* is interpreted as triggered by an intense precipitation event at 9230 cal BP, which is consistent with a period of weak westerly flow in the southern Hemisphere (11,000–8000 cal BP; Fletcher and Moreno, 2012) as well as pollen-based paleoprecipitation proxy from Laguna Potrok Aike (Schäbitz et al., 2013) and the Magellan Strait region (McCulloch et al., 2000).

Three pedogenic layers, *d*, *e*, and *f*, were not deposited during the periods of higher lacustrine productivity. Yet, high values of the degree of anisotropy as well as local intermediate values of productivity are associated with pedogenic events *e* and *f* (Fig. 10). This coincidence suggests that the crystalline or shape anisotropy of hematite/goethite particles might as well contribute to anisotropy together with biogenic magnetite.

Events *d* and *e* (Table 2) follow two major glacial advances of the PIS in the Magellanes Strait at 23,100–25,600 cal BP and 20,400–21,700 (Sugden et al., 2009). While the runoff event *d* is the only pedogenic layer that is not associated with a previously documented warm period, the event *e* and *f* at 24,280 and 30,640 cal BP, respectively, are coeval with the warm period AIM2 and AIM4 in Dronning Maud Land, Antarctica (Fig. 8; EPICA community members, 2006). Interestingly, a continental record from New Zealand similarly points to warmer temperatures during AIM2 as indicated by greater tree abundance (Callard et al., 2013).

6. Conclusions

The high-resolution rock-magnetic study of the sediments deposited in Laguna Potrok Aike since 51,200 cal BP indicates the presence of PSD magnetite with isolated intervals of iron sulfides (facies 1) and oxidized pedogenic particles (facies 2) representing a total of ca 5% of the sedimentary sequence. The two distinct types of magnetic signatures are associated with MMDs in Laguna Potrok Aike and display contrasting rock-magnetic signatures compared to the rest of the record dominated by PSD magnetite (Gogorza et al., 2011, 2012; Recasens et al., 2012; Lisé-Pronovost et al., 2013).

This study reveals that changes in the magnetic mineralogy are useful for identifying MMD in hydrologically closed lake basins with a uniform sediment source such as in the case of Laguna Potrok Aike. In particular, we used spurious laboratory magnetizations as a useful means of identifying the sedimentary magnetic mineralogy. While GRM is well-documented for iron sulfides (as in facies 1), we have provided evidence of GRM acquisition during AF demagnetization of IRM most likely attributed to pedogenic hematite (facies 2). In the rock-magnetic facies 1, iron sulfides are authigenically formed by sulfate reduction within MMD composed of mafic sand or tephra material. Facies 2 contains oxidized pedogenic iron minerals (such as hematite and goethite) formed in the lake catchment and transported to the lake by runoff events. Interestingly, a similar series of events characterized by high coercivity minerals and possibly attributed to pedogenized material during the Last Glacial period was reported in the sediment sequence of the oligotrophic maar lake Massoko in Tasmania (Williamson et al., 1999), hinting at a possibly common formation and deposition process in volcanic field settings. In Laguna Potrok Aike, the pedogenic particles were deposited on top of a MMD horizons at times of increased lacustrine productivity, higher MMD frequency, and increased gustiness, which are nowadays climatic conditions associated to the enhanced influence of humid air masses from the Atlantic Ocean (Ohlendorf et al., 2013; Schäbitz et al., 2013). Such paleoclimatic conditions during the Last Glacial period support the importance of gustiness (McGee et al., 2010). The coincidence of these major precipitation/melt events with the warm periods AIM-2, -4, -8 and -12 recorded in Antarctica (EPICA community members, 2006) reveals an Antarctic-like climate in south-eastern Argentina. The rock-magnetic results also provide evidence for permafrost melt at ca 50,000, 46,000 and 17,300 cal BP in the lake catchment of Laguna Potrok Aike. This work documents abrupt climate changes of regional and hemispheric significance.

Acknowledgments

We thank J. Labrie, F. Barletta, M.-P. St-Onge, A. Leclerc and D. Veres for their help in the laboratory at ISMER, J.J. Scagliotti and C. Ohlendorf for cube sampling at the University of Bremen, and M. Jackson for his help with anisotropy measurements at the Institute of Rock Magnetism of the University of Minnesota in Minneapolis. We thank Q. Simon, S. Brachfeld, A. Chauvin and an anonymous reviewer for comments on an earlier version of this manuscript. This research is supported by the International Continental Scientific Drilling Program (ICDP) in the framework of the "Potrok Aike Maar Lake Sediment Archive Drilling Project" (PASADO). Funding for drilling was provided by the ICDP, the German Science Foundation (DFG), the Swiss National Funds (SNF), the Natural Sciences and Engineering Research Council of Canada (NSERC), the Swedish Vetenskapsradet (VR) and the University of Bremen. For their invaluable help in field logistics and drilling, we thank the staff of INTA Santa Cruz and Rio Dulce Catering as well as the Moreteau family and the DOSECC crew. This research was made possible through NSERC Special Research Opportunity and Discovery grants to P. Francus and G. St-Onge. We also acknowledge the Canadian Foundation for Innovation (CFI) for the acquisition and operation of the u-channel cryogenic magnetometer. C. Gogorza thanks the *Comisión Nacional de Investigaciones Científicas y Técnicas de la República Argentina* (CONICET) and the *Universidad Nacional del*

Centro de la Provincia de Buenos Aires (UNCPBA). Finally, we acknowledge the support of NSERC and the Canadian Meteorological and Oceanographical Society (CMOS) for graduate scholarships to A. Lisé-Pronovost.

Appendix A. Supplementary data

Supplementary data related to this article can be found at http://dx.doi.org/10.1016/j.quascirev.2014.05.029.

References

Anderson, R.F., Ali, S., Bradtmiller, L.I., Nielsen, S.H.H., Fleisher, M.Q., Anderson, B.E., Burckle, L.H., 2009. Wind-driven upwelling in the southern ocean and the deglacial rise in atmospheric CO_2. Science 323 (5920), 1443–1448.

Anselmetti, F., Ariztegui, D., De Batist, M., Gebhardt, C., Haberzettl, T., Niessen, F., Ohlendorf, C., Zolitschka, B., 2009. Environmental history of southern Patagonia unraveled by the seismic stratigraphy of Laguna Potrok Aike. Sedimentology 56, 873–892.

Barrows, T.T., Juggins, S., De Deckker, P., Calvo, E., Pelejero, C., 2007. Long-term sea surface temperature and climate change in the Australian-New Zealand region: Australian-New Zealand climate change. Paleoceanography 22 (2), PA2215.

Basile, I., Grousset, F.E., Revel, M., Petit, J.R., Biscaye, P.E., Barkov, N.I., 1997. Patagonian origin of glacial dust deposited in East Antarctica (Vostok andDome C) during glacial stages 2, 4 and 6. Earth Planet. Sci. Lett. 146, 573–589.

Berner, R.A., 1984. Sedimentary pyrite formation: an update. Geochim. Cosmochim. Acta 48, 605–615.

Blanchet, C.L., Thouveny, N., Vidal, L., 2009. Formation and preservation of greigite (Fe_3 S_4) in sediments from the Santa Barbara Basin: implications for paleoenvironmental changes during the past 35 ka: greigite in Santa Barbara Basin. Paleoceanography 24, PA2224.

Blodau, C., Gatzek, C., 2006. Chemical controls on iron reduction in schwertmannite-rich sediments. Chem. Geol. 235, 366–376.

Blunier, T., Brook, E.J., 2001. Timing of millennial-scale climate change in Antarctica and Greenland during the Last Glacial Period. Science 291, 109.

Bockheim, J., Coronato, A., Rabassa, J., Ercolano, B., Ponce, J., 2009. Relict sand wedges in southern Patagonia and their stratigraphic and paleo-environmental significance. Quat. Sci. Rev. 28, 1188–1199.

Bowen, B.B., Benison, K.C., Oboh-Ikuenobe, F.E., Story, S., Mormile, M.R., 2008. Active hematite concretion formation in modern acid saline lake sediments, Lake Brown, Western Australia. Earth Planet. Sci. Lett. 268, 52–63.

Brachfeld, S., Barletta, F., St-Onge, G., Darby, D., Ortiz, J.D., 2009. Impact of diagenesis on the environmental magnetic record from a Holocene sedimentary sequence from the Chukchi–Alaskan margin, Arctic Ocean. Glob. Planet. Change 68, 100–114.

Brachfeld, S.A., 2006. High-field magnetic susceptibility (χHF) as a proxy of biogenic sedimentation along the Antarctic Peninsula. Phys. Earth Planet. Inter. 156, 274–282.

Callard, S.L., Newnham, R.M., Vandergoes, M.J., Alloway, B.V., Smith, C., 2013. The vegetation and climate during the Last Glacial Cold Period, northern South Island, New Zealand. Quat. Sci. Rev. 74, 230–244.

Caniupán, M., Lamy, F., Lange, C.B., Kaiser, J., Arz, H., Kilian, R., Baeza Urrea, O., Aracena, C., Hebbeln, D., Kissel, C., Laj, C., Mollenhauer, G., Tiedemann, R., 2011. Millennial-scale sea surface temperature and Patagonian Ice Sheet changes off southernmost Chile (53°S) over the past ~60 kyr. Paleoceanography 26, PA3221.

Carter-Stiglitz, B., Banerjee, S.K., Gourlan, A., Oches, E., 2006. A multi-proxy study of Argentina loess: Marine oxygen isotope stage 4 and 5 environmental record from pedogenic hematite. Paleogeogr. Palaeoclimatol. Palaeoecol. 239, 45–62.

Channell, J.E.T., Xuan, C., 2009. Self-reversal and apparent magnetic excursions in Arctic sediments. Earth Planet. Sci. Lett. 284, 124–131.

Coronato, A., Ercolano, B., Corbella, H., Tiberi, P., 2013. Glacial, fluvial and volcanic landscape evolution in the Laguna Potrok Aike maar area, Southern Patagonia, Argentina. Quat. Sci. Rev. 71, 13–26.

D'Orazio, M., Agostini, S., Mazzarini, F., Innocenti, F., Manetti, P., Haller, M.J., Lahsen, A., 2000. The Pali Aike volcanic field, Patagonia: slab-window magmatism near the tip of South America. Tectonophysics 321, 407–427.

Day, R., Fuller, M., Schmidt, V.A., 1977. Hysteresis properties of titano-magnetite: grain size and compositional dependence. Phys. Earth Planet. Inter. 13, 260–267.

Dearing, J.A., 1999. Environmental Magnetic Susceptibility: Using the Bartington MS2 System. Chi Pub., Kenilworth.

Dekkers, M.J., 1989. Magnetic properties of natural pyrrhotite. II. High- and low-temperature behaviour of Jrs and TRM as a function of grain size. Phys. Earth Planet. Inter. 57, 266–283.

Dekkers, M.J., 1997. Environmental magnetism: an introduction. Geol. Mijnb. 76, 163–182.

Dunlop, D.J., 2002. Theory and application of the Day plot (Mrs/Ms versus Hcr/Hc) 1. Theoretical curves and tests using titanomagnetite data. J. Geophys. Res. 107 (B3), 1–22.

Dunlop, D.J., Özdemir, O., 2007. Magnetizations in rocks and minerals. In: Schubert, G. (Ed.), Geomagnetism, Treatise on Geophysics, vol. 5. Elsevier, pp. 277–336.

Eden, D.N., Page, M.J., 1998. Palaeoclimatic implications of a storm erosion record from late Holocene lake sediments, North Island, New Zealand. Palaeogeogr. Palaeoclim. Palaeoecol. 139, 37–58.

Egli, R., 2004a. Characterization of individual rock magnetic components by analysis of remanence curves. 1. Unmixing natural sediments. Stud. Geophys. Geod. 48, 391–446.

Egli, R., 2004b. Characterization of individual rock magnetic components using the analysis of remanence curves, 3. Biogenic magnetite and natural processes in lakes. Phys. Chem. Earth 29, 869–884.

EPICA community members, 2006. One-to-one coupling of glacial climate variability in Greenland and Antarctica. Nature 444, 195–198.

Evans, M.E., Heller, F., 2003. Environmental magnetism: principles and applications of enviromagnetics. In: International Geophysics Series, vol. 86. Academic Press, 299 p.

Fletcher, M.-S., Moreno, P.I., 2012. Have the Southern Westerlies changed in a zonally symmetric manner over the last 14,000 years? A hemisphere-wide take on a controversial problem. Quat. Int. 253, 32–46.

Frankel, R.B., Bazylinski, D.A., 2003. Biologically induced mineralization by bacteria (in Biomineralization). Rev. Mineral. Geochem. 54, 95–114.

Fu, Y., von Dobeneck, T., Franke, C., Heslop, D., Kasten, S., 2008. Rock magnetic identification and geochemical process models of greigite formation in Quaternary marine sediments from the Gulf of Mexico (IODP Hole U1319A). Earth Planet. Sci. Lett. 275, 233–245.

Garreaud, R., Lopez, P., Minvielle, M., Rojas, M., 2013. Large scale control on the Patagonia climate. J. Clim. 26, 215–230.

Gasse, F., Chalié, F., Vincens, A., Williams, A.J., Williamson, D., 2008. Climatic patterns in equatorial and southern Africa from 30,000 to 10,000 years ago reconstructed from terrestrial and near-shore proxy data. Quat. Sci. Rev. 27, 2316–2340.

Gobeil, C., Macdonald, R.W., Sundby, B., 1997. Diagenetic separation of cadmium and manganese in suboxic continental margin sediments. Geochim. Cosmochim. Acta 61, 4647–4654.

Gogorza, C.S.G., Irurzun, M.A., Sinito, A.M., Lisé-Pronovost, A., St-Onge, G., Haberzettl, T., Ohlendorf, C., Kastner, S., Zolitschka, B., 2012. High-resolution paleomagnetic records from Laguna Potrok Aike (Patagonia, Argentina) for the last 16,000 years. Geochem. Geophys. Geosyst. 13, Q12Z37.

Gogorza, C.S.G., Sinito, A.M., Ohlendorf, C., Kastner, S., Zolitschka, B., 2011. Paleosecular variation and paleointensity records for the last millennium from southern South America (Laguna Potrok Aike, Santa Cruz, Argentina). Phys. Earth Planet. Inter. 184, 41–50.

Haberzettl, T., Anselmetti, F.S., Bowen, S.W., Fey, M., Mayr, C., Zolitschka, B., Ariztegui, D., Mauz, B., Ohlendorf, C., Kastner, S., Lücke, A., Schäbitz, F., Wille, M., 2009. Late Pleistocene dust deposition in the Patagonian steppe – extending and refining the paleoenvironmental and tephrochronological record from Laguna Potrok Aike back to 55ka. Quat. Sci. Rev. 28, 2927–2939.

Haberzettl, T., Kück, B., Wulf, S., Anselmetti, F., Ariztegui, D., Corbella, H., Fey, M., Janssen, S., Lücke, A., Mayr, C., Ohlendorf, C., Schäbitz, F., Schleser, G.H., Wille, M., Zolitschka, B., 2008. Hydrological variability in southeastern Patagonia and explosive volcanic activity in the southern Andean Cordillera during Oxygen Isotope Stage 3 and the Holocene inferred from lake sediments of Laguna Potrok Aike, Argentina. Palaeogeogr. Palaeoclim. Palaeoecol. 259, 213–229.

Haberzettl, T., Corbella, H., Fey, M., Janssen, S., Lucke, A., Mayr, C., Ohlendorf, C., Schabitz, F., Schleser, G.H., Wille, M., Wulf, S., Zolitschka, B., 2007. Lateglacial and Holocene wet-dry cycles in southern Patagonia: chronology, sedimentology and geochemistry of a lacustrine record from Laguna Potrok Aike, Argentina. Holocene 17, 297–310.

Haberzettl, T., Fey, M., Lücke, A., Maidana, N., Mayr, C., Ohlendorf, C., Schäbitz, F., Schleser, G.H., Wille, M., Zolitschka, B., 2005. Climatically induced lake level changes during the last two millennia as reflected in sediments of Laguna Potrok Aike, southern Patagonia (Santa Cruz, Argentina). J. Paleolimnol. 33, 283–302.

Hahn, A., Kliem, P., Ohlendorf, C., Zolitschka, B., Rosén, P., 2013. Climate induced changes as registered in inorganic and organic sediment components from Laguna Potrok Aike (Argentina) during the past 51 ka. Quat. Sci. Rev. 71, 154–166.

Hahn, A., Kliem, P., Oehlerich, M., Ohlendorf, C., Zolitschka, B., the PASADO Science Team, 2014. Elemental composition of Laguna Potrok Aike sediment sequence reveals paleoclimate change over the past 51 ka in southern Patagonia, Argentina. (submitted for publication).

Horng, C.-S., Roberts, A.P., 2006. Authigenic or detrital origin of pyrrhotite in sediments? Resolving a paleomagnetic conundrum. Earth Planet. Sci. Lett. 241, 750–762.

Hu, S., Stephenson, A., Appel, E., 2002. A study of gyroremanent magnetisation (GRM) and rotational remanent magnetisation (RRM) carried by greigite from lake sediments. Geophys. J. Int. 151, 469–474.

Hu, S., Appel, E., Hoffmann, V., Schmahl, W.W., Wang, S., 1998. Gyromagnetic remanence acquired by greigite (Fe3S4) during static three-axis alternating field demagnetization. Geophys. J. Int. 134, 831–842.

Jouve, G., Francus, P., De Coninck, A., Bouchard, F., Lamoureux, S.F., the PASADO Science Team, 2014. microsedimentological investigations in lacustrine sediments from a maar lake: implications for paleoenvironmental reconstructions. J. Paleolimnol. (submitted for publication).

Jouve, G., Francus, P., Lamoureux, S., Provencher-Nolet, L., Hahn, A., Haberzettl, T., Fortin, D., Nuttin, L., 2013. Microsedimentological characterization using image analysis and μ-XRF as indicators of sedimentary processes and climate changes during Lateglacial at Laguna Potrok Aike, Santa Cruz, Argentina. Quat. Sci. Rev. 71, 191–204.
Kaiser, J., Lamy, F., Arz, H.W., Hebbeln, D., 2007. Dynamics of the millennial-scale sea surface temperature and Patagonian Ice Sheet fluctuations in southern Chile during the last 70kyr (ODP Site 1233). Quat. Int. 161, 77–89.
Kilian, R., Lamy, F., 2012. A review of Glacial and Holocene paleoclimate records from southernmost Patagonia (49–55°S). Quat. Sci. Rev. 53, 1–23.
Kilian, R., Schneider, C., Koch, J., Fesq-Martin, M., Biester, H., Casassa, G., Arévalo, M., Wendt, G., Baeza, O., Behrmann, J., 2007. Palaeoecological constraints on late Glacial and Holocene ice retreat in the Southern Andes (53°S). Glob. Planet. Change 59, 49–66.
King, J.W., Banerjee, S.K., Marvin, J.A., Özdemir, Ö., 1982. A comparison of different magnetic methods for determining the relative grain size of magnetite in natural materials: some results from lake sediments. Earth Planet. Sci. Lett. 59, 404–419.
Kliem, P., Enters, D., Hahn, A., Ohlendorf, C., Lisé-Pronovost, A., St-Onge, G., Wastegård, S., Zolitschka, B., 2013a. Lithology, radiocarbon chronology and sedimentological interpretation of the lacustrine record from Laguna Potrok Aike, southern Patagonia. Quat. Sci. Rev. 71, 54–69.
Kliem, P., Buylaert, J.P., Hahn, A., Mayr, C., Murray, A.S., Ohlendorf, C., Veres, D., Wastegård, S., Zolitschka, B., 2013b. Magnitude, geomorphologic response and climate links of lake level oscillations at Laguna Potrok Aike, Patagonian steppe (Argentina). Quat. Sci. Rev. 71, 131–146.
Knorr, G., Lohmann, G., 2003. Southern Ocean origin for the resumption of Atlantic thermohaline circulation during deglaciation. Nature 424, 532–536.
Konhauser, K.O., 1998. Diversity of bacterial iron mineralization. Earth-Sci. Rev. 43, 91–121.
Larrasoaña, J.C., Roberts, A.P., Musgrave, R.J., Gràcia, E., Piñero, E., Vega, M., Martínez-Ruiz, F., 2007. Diagenetic formation of greigite and pyrrhotite in gas hydrate marine sedimentary systems. Earth Planet. Sci. Lett. 261, 350–366.
Lascu, I., Plank, C., 2013. A new dimension to sediment magnetism: charting the spatial variability of magnetic properties across lake basins. Glob. Planet. Change 110 (part C), 340–349.
Lisé-Pronovost, A., St-Onge, G., Gogorza, C., Haberzettl, T., Jouve, G., Francus, P., Zolitschka, B., the PASADO Science Team, 2014. Rock-magnetic proxy of wind intensity and dust since 51200 cal BP from the sediments of Laguna Potrok Aike in southern Patagonia. (submitted for publication).
Lisé-Pronovost, A., St-Onge, G., Gogorza, C., Haberzettl, T., Preda, M., Kliem, P., Francus, P., Zolitschka, B., 2013. High-resolution paleomagnetic secular variations and relative paleointensity since the Late Pleistocene in southern South America. Quat. Sci. Rev. 71, 91–108.
Liu, Q., Barrón, V., Torrent, J., Qin, H., Yu, Y., 2010. The magnetism of micro-sized hematite explained. Phys. Earth Planet. Inter. 183, 387–397.
Maher, B.A., 2011. The magnetic properties of Quaternary aeolian dusts and sediments, and their palaeoclimatic significance. Aeolian Res. 3, 87–144.
Maher, B.A., Alekseev, A., Alekseeva, T., 2003. Magnetic mineralogy of soils across the Russian Steppe: climatic dependence of pedogenic magnetite formation. Palaeogeogr. Palaeoclim. Palaeoecol. 201, 321–341.
Maher, B.A., Thompson, R., 1999. Quaternary Climates, Environments, and Magnetism. Cambridge University Press, Cambridge, UK; New York.
Maher, B.A., Thompson, R., Hounslow, M.W., 1999. In: Maher and Thompson Quaternary Climates, Environments and Magnetism. Cambridge University Press, 412 p.
Maher, B.A., 1988. Magnetic properties of some synthetic sub-micron magnetites. Geophys. J 94, 83–96.
Maher, B.A., Taylor, R.M., 1988. Formation of ultrafine-grained magnetite in soils. Nature 336, 368–370.
Maher, B.A., 1998. Magnetic properties of modern soils and Quaternary loessic paleosols: paleoclimatic implications. Palaeogeogr. Palaeoclim. Palaeoecol. 137, 25–54.
Mayr, C., Lücke, A., Stichler, W., Trimborn, P., Ercolano, B., Oliva, G., Ohlendorf, C., Soto, J., Fey, M., Haberzettl, T., Janssen, S., Schäbitz, F., Schleser, G.H., Wille, M., Zolitschka, B., 2007. Precipitation origin and evaporation of lakes in semi-arid Patagonia (Argentina) inferred from stable isotopes (δ18O, δ2H). J. Hydrol. 334, 53–63.
Mazaud, A., Kissel, C., Laj, C., Sicre, M.A., Michel, E., Turon, J.L., 2007. Variations of the ACC-CDW during MIS3 traced by magnetic grain deposition in midlatitude South Indian Ocean cores: connections with the northern hemisphere and with central Antarctica. Geochem. Geophys. Geosyst. 8 (5), Q05012.
McCulloch, R.D., Bentley, M.J., Purves, R.S., Hulton, N.R.J., Sudgen, D.E., Clapperton, C.M., 2000. Climatic inferences from glacial and palaeoecological evidence at the last glacial termination, southern South America. J. Quat. Sci. 15 (4), 409–417.
McGee, D., Broecker, W.S., Winckler, G., 2010. Gustiness: the driver of glacial dustiness? Quat. Sci. Rev. 29, 2340–2350.
Moskowitz, B.M., Frankel, R.B., Bazylinski, D.A., 1993. Rock magnetic criteria for the detection of biogenic magnetite. Earth Planet. Sci. Lett. 120, 283–300.
Muxworthy, A.R., Roberts, A.P., 2007. First-order reversal curve (FORC) diagrams. In: Gubbins, D., Herrero-Bervera, E. (Eds.), Encyclopedia of Geomagnetism and Paleomagnetism. Springer, Dordrecht, Netherlands, pp. 266–272.
Nuttin, L., Francus, P., Preda, M., Ghaleb, B., Hillaire-Marcel, C., 2013. Authigenic, detrital and diagenetic minerals in the Laguna Potrok Aike sediment sequence. Quat. Sci. Rev. 71, 109–118.
Ohlendorf, C., Fey, M., Gebhardt, C., Haberzettl, T., Lücke, A., Mayr, C., Schäbitz, F., Wille, M., Zolitschka, B., 2013. Mechanisms of lake-level change at Laguna Potrok Aike (Argentina) – insights from hydrological balance calculations. Quat. Sci. Rev. 71, 27–45.
Özdemir, Ö., Banerjee, S.K., 1982. A preliminary magnetic study of soil samples from west central Minnesota. Earth Planet. Sci. Lett. 59, 393–403.
Pahnke, K., 2003. 340,000-Year centennial-scale marine record of Southern Hemisphere climatic oscillation. Science 301, 948–952.
Potter, D.K., Stephenson, A., 2006. The stable orientations of the net magnetic moment within single-domain particles: experimental evidence for a range of stable states and implications for rock magnetism and palaeomagnetism. Phys. Earth Planet. Inter. 154, 337–349.
Pugh, R.S., McCave, I.N., Hillenbrand, C.-D., Kuhn, G., 2009. Circum-Antarctic age modelling of Quaternary marine cores under the Antarctic Circumpolar Current: ice-core dust–magnetic correlation. Earth Planet. Sci. Lett. 284, 113–123.
Recasens, C., Ariztegui, D., Gebhardt, C., Gogorza, C., Haberzettl, T., Hahn, A., Kliem, P., Lisé-Pronovost, A., Lücke, A., Maidana, N., 2012. New insights into paleoenvironmental changes in Laguna Potrok Aike, southern Patagonia, since the Late Pleistocene: the PASADO multiproxy record. Holocene 22, 1323–1335.
Roberts, A.P., 2006. High-resolution magnetic analysis of sediment cores: strengths, limitations and strategies for maximizing the value of long-core magnetic data. Phys. Earth Planet. Inter. 156, 162–178.
Roberts, A.P., 1995. Magnetic properties of sedimentary greigite (Fe3S4). Earth Planet. Sci. Lett. 134, 227–236.
Roberts, A.P., Chang, L., Rowan, C.J., Horng, C.-S., Florindo, F., 2011. Magnetic properties of sedimentary greigite (Fe_3S_4): an update. Rev. Geophys 49.
Roberts, A., Pike, C.R., Verosub, K.L., 2000. First-order reversal curve diagrams: a new tool for characterizing the magnetic properties of natural samples. J. Geophys. Res. 105 (B12), 28,461–28,475.
Roberts, A.P., Liu, Q., Rowan, C.J., Chang, L., Carvallo, C., Torrent, J., Horng, C.-S., 2006. Characterization of hematite (α–Fe_2O_3), goethite (α-FeOOH), greigite (Fe_3S_4), and pyrrhotite (Fe_7S_8) using first-order reversal curve diagrams. J. Geophys. Res. 111.
Robinson, S.G., 2000. Early disgenesis in an organic-rich turbidite and pelagic clay sequence from the Cape Verde Abyssal Plain, NE Atlantic: magnetic and geochemical signals. Sediment. Geol. 143, 91–123.
Rochette, P., Mathé, P.-E., Esteban, L., Rakoto, H., Bouchez, J.-L., Liu, Q., Torrent, J., 2005. Non-saturation of the defect moment of goethite and fine-grained hematite up to 57 Teslas. Geophys. Res. Lett. 32.
Roperch, P., Taylor, G.K., 1986. The importance of gyromagnetic remanence in alternating field demagnetization. Some new data and experiments on G.R.M. and R.R.M. Geophys. J. R. Astr. Soc. 87, 949–965.
Roperch, P., Chauvin, A., Valdez, F., 2012. Partial self-reversal of TRM in baked soils and ceramics from Ecuador. Phys. Earth Planet. Inter. 210–211, 8–20.
Ross, P.-S., Delpit, S., Haller, M.J., Németh, K., Corbella, H., 2011. Influence of the substrate on maar–diatreme volcanoes — an example of a mixed setting from the Pali Aike volcanic field, Argentina. J. Volcanol. Geotherm. Res. 201, 253–271.
Sagnotti, L., 2007. Iron sulphides. In: Gubbins, Herrero-Bervera (Eds.), Encyclopedia of Geomagnetism and Paleomagnetism.
Sagnotti, L., Winkler, A., 1999. Rock magnetism and palaeomagnetism of greigite-bearing mudstones in the Italian peninsula. Earth Planet. Sci. Lett. 165, 67–80.
Schäbitz, F., Wille, M., Francois, J.-P., Haberzettl, T., Quintana, F., Mayr, C., Lücke, A., Ohlendorf, C., Mancini, V., Paez, M.M., Prieto, A.R., Zolitschka, B., 2013. Reconstruction of palaeoprecipitation based on pollen transfer functions – the record of the last 16 ka from Laguna Potrok Aike, southern Patagonia. Quat. Sci. Rev. 71, 175–190.
Schaefer, J.M., 2006. Near-synchronous interhemispheric termination of the Last Glacial Maximum in mid-latitudes. Science 312, 1510–1513.
Schwertmann, U., Murad, E., Schulze, D.G., 1982. Is there Holocene reddening (hematite formation) in soils of axeric temperature climates? Geoderma 27, 209–223.
Schwertmann, U., 2008. Iron oxides. In: Chesworth, W. (Ed.), Encyclopedia of Soil Science, p. 902.
Snowball, I., 1991. Magnetic hysteresis properties of greigite (Fe_3S_4) and a new occurrence in Holocene sediments from Swedish Lappland. Phys. Earth Planet. Inter. 68, 32–40.
Snowball, I.F., 1997. Gyroremanent magnetization and the magnetic properties of greigite-bearing clays in southern Sweden. Geophys. J. Int. 129, 624–636.
Snowball, I.F., Thompson, R., 1990. A stable chemical remanence in Holocene sediments,. J. Geophys. Res. 95, 4471–4479.
Snowball, I., Zillen, L., Sandgren, P., 2002. Bacterial magnetite in Swedish varved lake-sediments: a potential bio-marker of environmental change. Quat. Int. 88, 13–19.
Stephenson, A., 1980. A gyroremanent magnetization in anisotropic magnetic material,. Nature 284, 49–51.
Stephenson, A., Snowball, I.F., 2001. A large gyromagnetic effect in greigite. Geophys. J. Int. 145, 570–575.
Stoner, J.S., St-Onge, G., 2007. Chapter three. Magnetic stratigraphy in paleoceanography: reversals, excursions, paleointensity, and secular variation. In: Developments in Marine Geology. Elsevier, pp. 99–138.
Stoner, J.S., Channell, J.E.T., Hillaire-Marcel, C., 1996. The magnetic signature of rapidly deposited detrital layers from the deep Labrador Sea: relationship to North Atlantic Heinrich layers. Paleoceanography 11 (3), 309–325.
Stumm, W., Morgan, J.J., 1996. Chemical Equilibria and Rates in Natural Waters, third ed. John Wiley & Sons, Inc., New York, p. 1022.

Sugden, D.E., McCulloch, R.D., Bory, A.J.-M., Hein, A.S., 2009. Influence of Patagonian glaciers on Antarctic dust deposition during the last glacial period. Nat. Geosci. 2, 281–285.
Tauxe, L., 2010. Essentials of Paleomagnetism. Univ. Of Calif. Press, San Diego, 513 p.
Tauxe, L., Constable, C.G., Stokking, L.B., Badgley, C., 1990. The use of anisotropy to determine the origin of characteristic remanence in the Siwalik red beds of northern Pakistan. J. Geophys. Res. 95, 4391–4404.
Tauxe, L., Mullender, T.A.T., Pick, T., 1996. Potbellies, wasp-waists, and superparamagnetism in magnetic hysteresis. J. Geophys. Res. 101 (B1), 571–583.
Thompson, R., Oldfield, F., 1986. Environmental Magnetism. Allen & Unwin, London.
Verosub, K.L., Roberts, A.P., 1995. Environmental magnetism: past, present, and future. J. Geophys. Res. 100 (B2), 2175–2192.
Vogt, T., Larqué, P., 2002. Clays and secondary minerals as permafrost indicators: examples from the circum-Baikal region. Quat. Int. 95, 175–187.
Vuillemin, A., Ariztegui, D., De Coninck, A.S., Lucke, A., Mayr, C., Schubert, C.J., the PASADO Scientific Team, 2013. Origin and significance of diagenetic concretions in sediments of Laguna Potrok Aike, southern Argentina. J. Paleolimnol. 50, 275–291.
Wastegård, S., Veres, D., Kliem, P., Hahn, A., Ohlendorf, C., Zolitschka, B., 2013. Towards a late Quaternary tephrochronological framework for the southernmost part of South America – the Laguna Potrok Aike tephra record. Quat. Sci. Rev. 71, 81–90.
Weber, M.E., Kuhn, G., Sprenk, D., Rolf, C., Ohlwein, C., Ricken, W., 2012. Dust transport from Patagonia to Antarctica – a new stratigraphic approach from the Scotia Sea and its implications for the last glacial cycle. Quat. Sci. Rev. 36, 177–188.
Wehland, F., Stancu, A., Rochette, P., Dekkers, M.J., Appel, E., 2005. Experimental evaluation of magnetic interaction in pyrrhotite bearing samples. Phys. Earth Planet. Inter. 153, 181–190.
Wille, M., Maidana, N.I., Schäbitz, F., Fey, M., Haberzettl, T., Janssen, S., Lücke, A., Mayr, C., Ohlendorf, C., Schleser, G.H., Zolitschka, B., 2007. Vegetation and climate dynamics in southern South America: the microfossil record of Laguna Potrok Aike, Santa Cruz. Argent. Rev. Palaeobot. Palynol. 146, 234–246.
Williams, M., Cook, E., van der Kaars, S., Barrows, T., Shulmeister, J., Kershaw, P., 2009. Glacial and deglacial climatic patterns in Australia and surrounding regions from 35 000 to 10 000 years ago reconstructed from terrestrial and near-shore proxy data. Quat. Sci. Rev. 28, 2398–2419.
Williamson, D., Jackson, M.J., Banerjee, S.K., Marvin, J., Merdaci, O., Thouveny, N., Decobert, M., Gibert-Massault, E., Massault, M., Mazaudier, D., Taieb, M., 1999. Magnetic signatures of hydrological change in a tropical Maar-Lake (Lake Massoko, Tanzania): preliminary results. Phys. Chem. Earth (A) 24 (9), 799–803.
Zolitschka, B., Anselmetti, F., Ariztegui, D., Corbella, H., Francus, P., Lücke, A., Maidana, N., Ohlendorf, C., Schäbitz, F., Wastegård, S., 2013. Environment and climate of the last 51,000 years – new insights from the Potrok Aike maar lake Sediment Archive Drilling prOject (PASADO). Quat. Sci. Rev. 71, 1–12.
Zolitschka, B., Anselmetti, F., Ariztegui, D., Corbella, H., Francus, P., Ohlendorf, C., Schäbitz, the P.S.D.T, 2009. The Laguna Potrok Aike Scientific Drilling Project PASADO (ICDP Expedition 5022). Sci. Drill. 8, 29–34.
Zolitschka, B., Schäbitz, F., Lücke, A., Corbella, H., Ercolano, B., Fey, M., Haberzettl, T., Janssen, S., Maidana, N., Mayr, C., Ohlendorf, C., Oliva, G., Paez, M.M., Schleser, G.H., Soto, J., Tiberi, P., Wille, M., 2006. Crater lakes of the Pali Aike Volcanic Field as key sites for paleoclimatic and paleoecological reconstructions in southern Patagonia, Argentina. J. South Am. Earth Sci. 21, 294–309.